STUK-YTO-TR 163 March 2000

# DECOVALEX II

The summary report of the Finnish contributions 1995–1999

**Esko Eloranta (ed.)**

STUK • SÄTEILYTURVAKESKUS • STRÅLSÄKERHETSCENTRALEN
RADIATION AND NUCLEAR SAFETY AUTHORITY

The conclusions presented in the STUK report series are those of the authors and do not necessarily represent the official position of STUK.

ISBN 951-712-379-5
ISSN 0785-9325

Oy Edita Ab, Helsinki 2000

*ELORANTA Esko (ed.). DECOVALEX II. The summary report of the Finnish contributions 1995–1999. STUK-YTO-TR 163. Helsinki 2000. 12 pp. + Appendices 26 pp.*

**ISBN** 951-712-379-5
**ISSN** 0785-9325

**Keywords:** rock mechanics, coupled processes, numerical modelling, spent fuel disposal

# ABSTRACT

During the years 1995–1999, an international effort was going on under the title DECOVALEX II, in order to study the coupled thermo-hydro-mechanical (THM) effects in the water containing fractured rock mass caused by the heat generation of spent fuel canisters in a repository. The project was a continuation project of DECOVALEX (1991–1995). The name comes from the acronym 'an international co-operative project for the DEvelopment of COupled models and their VALidation against EXperiments in nuclear waste isolation'. Radiation and Nuclear Safety Authority (STUK) was one of the eleven Funding Organizations in the international project. STUK's Research Team was the Technical Research Centre of Finland, VTT Communities and Infrastructure.

To support and coordinate the national research work, STUK formed a *National DECOVALEX II Group (NDG)*. The group had representatives from six research organizations and rock engineering firms interested in the field of coupled processes. The group gathered 13 time during the years 1996–1999.

The Finnish contribution was mainly concentrated on two topics. STUK continued the work related to the 'constitutive relationships of rock joints' begun already during DECOVALEX 1991–1995. This work belonged to Task 3 in the international project. The other topic was the hydromechanical response of the Sellafield (UK) shaft excavation, i.e. Task 1C of the international project.

This report summarizes the national work in DECOVALEX II during the years 1995–1999.

*ELORANTA Esko (toim.). DECOVALEX II. Yhteenveto Suomen kansallisesta tutkimuksesta 1995–1999. STUK-YTO-TR 163. Helsinki 2000. 12 s. + liitteet 26 s.*

**ISBN** 951-712-379-5
**ISSN** 0785-9325

**Avainsanat:** kalliomekaniikka, kytketyt prosessit, numeerinen mallintaminen, käytetyn ydinpolttoaineen loppusijoitus

# TIIVISTELMÄ

Vuosina 1995–1999 oli käynnissä kansainvälinen DECOVALEX II -projekti. Yleistavoitteena oli tutkia kytkettyjä termo-hydro-mekaanisia (THM) prosesseja rakoilleessa, vettä sisältävässä kalliossa. Projekti oli jatkoa vuosina 1991–1995 toimineelle DECOVALEX-projektille. Säteilyturvakeskus (STUK) oli DECOVALEX II -projektin yksi yhdestätoista rahoittavasta organisaatiosta. STUKin tutkimusryhmänä toimi VTT:n Yhdyskuntatekniikka.

Kansallisen tutkimuksen toteuttamista ja koordinointia varten STUK perusti *Kansallisen DECOVALEX II -ryhmän,* johon kuului kuusi aihepiiristä kiinnostunutta tutkimusorganisaatiota ja kalliotekniikan alan yritystä. Ryhmä kokoontui 13 kertaa vuosina 1996–1999.

Suomen osuuden kansainvälisessä projektissa muodosti rakojen konstitutiivisten mallien kehitystyö, joka kuului projektin Task 3:een. Toisena tehtävänä tarkasteltiin Sellafieldiin (Yhdistynyt Kuningaskunta) suunnitellun kuilun rakentamisen hydromekaanisia vaikutuksia, joka kuului Task 1C:n aihepiiriin.

Tässä raportissa esitetään yhteenveto Suomen kansallisesta tutkimuksesta DECOVALEX II -projektissa vuosina 1995–1999.

# CONTENTS

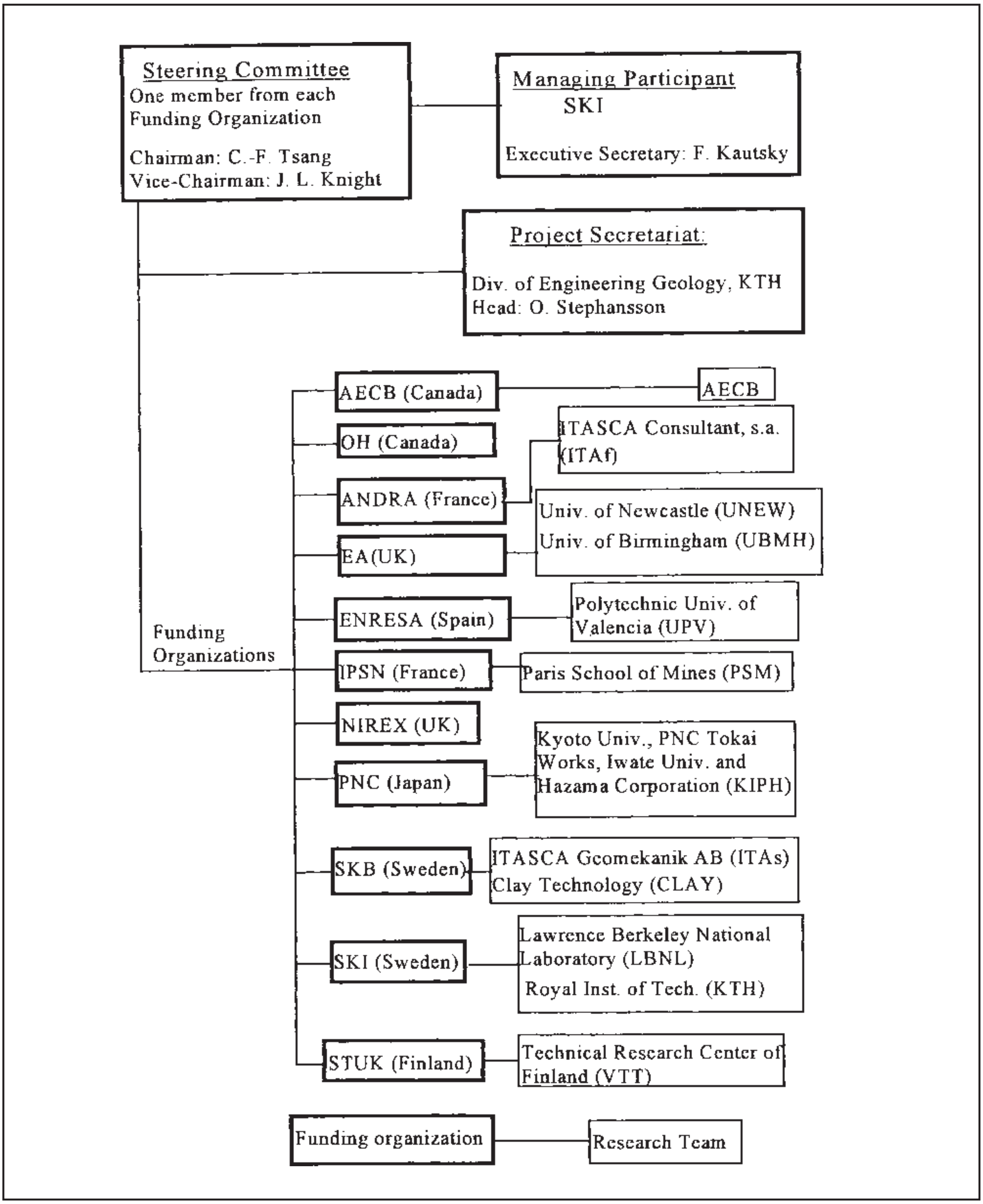


***Figure 1.*** *Organisation of DECOVALEX II, 1995–1999.*

# 1 INTRODUCTION

DECOVALEX II (an acronym for the International co-operative project for the **DE**velopment of **CO**upled models and their **VAL**idation against **EX**periments in nuclear waste isolation) was a continuation of the multi-disciplinary interactive and co-operative research effort in modelling Thermo – Hydro – Mechanical (THM) processes in fractured rocks and buffer materials going on since 1991 under the title DECOVALEX. DECOVALEX II was undertaken in 1995–1999.

The organization of DECOVALEX II is presented in Figure 1. The managing participant was the Swedish Nuclear Power Inspectorate (SKI). The Steering Committee was composed of the Funding Organizations of the project. Under the Funding Organizations or Parties (non-funding organization) there were the Research Teams (one or more per Funding Organization or Party) which performed the actual research work. At the end of the project in 1999 the following acted as Funding Organizations: Atomic Energy Control Board, AECB (Canada), Ontario Hydro, OH (Canada), Agence Nationale pour la Gestion des Déchets Radioactifs, ANDRA (France), Environmental Agency, EA (United Kingdom), Empresa Nacional de Residuos Radiactivos, S.A., ENRESA (Spain), Institut de Protection et de Sûreté Nucléaire, IPSN (France), United Kingdom Nirex Limited, NIREX (United Kingdom), Japan Nuclear Cycle Development Institute, JNC [formerly Power Reactor and Nuclear Fuel Development Corporation, PNC] (Japan), Swedish Nuclear Fuel and Waste Management Co., SKB (Sweden), Swedish Nuclear Power Inspectorate, SKI (Sweden), and Radiation and Nuclear Safety Authority, STUK (Finland). The division of Engineering Geology at the Royal Institute of Technology, KTH (Sweden) acted as the project Secretariat.

As can be seen on the above list there were participants from nuclear waste regulators (authorities) as well as from implementators.

Seven meetings and workshops have been arranged in different countries during the years 1995-1999. The start up meeting was in Oxford, UK, November 1995. The second workshop was in Tokyo, Japan, May 1996, the third in Cordoba, Spain, November 1996, the fourth in Toronto, Canada, June 1997, the fifth in Berkeley, USA, December 1997, the sixth in Avignon, France, June 1998, and the seventh in Kalmar, Sweden, March 1999.

This report concentrates only on the Finnish contributions to the international project without any comparisons of results with other research teams, review or ‘lessons learned’ options. Such issues are described in the documents of the international project which are referred to in the following chapter and which are listed in the references at the end of the present report.

# 2 THE TASKS OF DECOVALEX II

The general objective of DECOVALEX II was to increase the understanding of various thermo-hydro-mechanical (THM) processes of importance for radionuclide release and transport from a repository to the biosphere and how they can be described by mathematical models. DECOVALEX II had four Tasks. Two of these were based on large-scale *in-situ* experiments. The tasks were:

**Task 1.** Numerical study of Nirex's RCF Shaft excavation at Sellafield, UK. Simulation of the coupled hydro-mechanical processes of the RCF3 pumping test and responses of the rock mass to the shaft excavation, including study of the excavation induced disturbed zone (EDZ). The task was divided into three subtasks.

**Task 2.** Numerical study of PNC's *in-situ* THM experiments in Kamaishi Mine, Japan. An integrated investigation of a complete rock-buffer-heater system under *in-situ* conditions over a long period of time. The task was divided into three subtasks.

**Task 3.** Discussion and Peer Review of development of the constitutive relationships of rock joints.

**Task 4.** Preparation of statements on the state-of-science of coupled THM processes related to nuclear waste repository performance assessment.

The objectives were (1) to increase the basic understanding of THM coupled processes in fractured rocks and buffer materials, (2) to support the application of numerical models for THM modelling of jointed rocks and buffer material, (3) to investigate the predictive capabilities of different codes to field experiments and to perform verification of codes, (4) to exchange experimental data, and improve the understanding of the constitutive behaviour of rock joints, and (5) to prepare statements on the state-of-science in coupled THM issues for performance assessment.

The activities of the international project have been reported by SKI. The reader who is interested in the details of the DECOVALEX II project is recommended to read the present report in conjunction of the subsequently mentioned reports.

The project is characterized as a whole in an executive summary report (Jing, Stephansson, Tsang, Knight, and Kautsky 1999).

The subtasks of Task 1 – Task 1A and 1B - have been reported in (Jing, Stephansson, Tsang, Knight, and Kautsky 1998), and Task 1C in (Jing, Stephansson, Knight, Kautsky, and Tsang 1999).

The subtasks of Task 2 – Task 2A and 2B – have been reported in (Jing, Stephansson, Tsang, Chijimatsu and Kautsky, 1998), and Task 2C in (Jing, Stephansson, Börgesson, Chijimatzu, Kautsky, and Tsang 1999).

Task 4 has been reported in (Stephansson, Hudson, Tsang, Jing, and Andersson 1999).

Task 3 had no general international report because the issues were handled by national organizations which described their work at the workshops. This was also the situation with the Finnish work. The original approach of Task 3 was to organise special sessions at all workshops for invited presentations about rock discontinuities.

# 3 THE FINNISH CONTRIBUTIONS

When DECOVALEX II started in the autumn 1995 STUK made a decision that it will participate at the beginning as a non-funding organization in the project. VTT Communities and Infrastructure (and its predecessor VTT Road, Traffic and Geotechnical Laboratory) had been STUK's Research Team in DECOVALEX 1991-1995. A decision was made at STUK that the same Research Team can continue also in DECOVALEX II. STUK concentrated its activities on Task 3, i.e., constitutive relationships of rock joints.

STUK was a non-funding organization in 1996. From 1997 STUK participated in the project as a funding organization. In 1998 STUK and its Research Team, i.e. VTT Communities and Infrastructure, begun to work with Task 1, especially its subtask Task 1C, 'Prediction of hydro-mechanical response in Sector 7 of BVG due to shaft excavation'.

## 3.1 Task 3 'Constitutive relationships'

During the first DECOVALEX project in 1994–1995 an experimental compression test was made at the Laboratory of Rock Engineering of the Helsinki University of Technology. The aim was to study the flow properties of a single fracture under normal stress (Kuusela-Lahtinen et al. 1996, Pöllä et al. 1996). To continue this work fracture surface characterization (Vuopio and Pöllä 1997) and numerical modellings for water flow (Niemi 1999) were performed as parts of Task 3 for DECOVALEX II in 1996–1998. Niemi (1999) gathered the work done in the numerical flow modelling.

The report of Niemi (1999) includes two papers. Paper I is a conference paper presented in NYRocks'97 rock mechanics symposium in New York, USA in 1997. Its title is 'Simulation of heterogeneous flow in a natural fracture under varying normal stress'. Paper II is a progress report and it is titled as 'Generation of fracture surfaces and aperture distributions for Monte Carlo type hydraulic simulations'.

The reports (Vuopio and Pöllä 1997) and (Niemi 1999) have been published by STUK in the STUK-YTO-TR -series. So they are not reproduced in the present report.

## 3.2 Task 1C 'Prediction of hydro-mechanical responses in Sector 7 of BVG due to shaft excavation, Sellafield, UK'

The results of the numerical simulations of Task 1C have been documented by VTT Communities and Infrastructure. They are presented in the Appendix of the present report. The Appendix is composed of two Parts. Part I concerns the derivation of parameters and continuum simulations. Part II concerns the flow preditictions.

## 3.3 Task 4 'Coupled T-H-M issues related to repository design and performance'

The Finnish contribution to Task 4 was restricted to the review and comments on the report by Stephansson et al. (1999). The DECOVALEX II Steering Committee asked every Funding Organization to nominate one or more experts in Performance Assessment/Safety Assessment issues to give their comments on the report. For that purpose STUK formed a working group consisting of Dr. Timo Vieno from VTT Energy, and Dr. Aimo Hautojärvi from Posiva Oy to work with Task 4 statements. The working group gave their comments which were taken into account in the final report.

# 4 THE NATIONAL DECOVALEX II GROUP

To follow up the international DECOVALEX II project and to coordinate the national research work in Finland STUK formed a so called National DECOVALEX II Group (NDG). The group was similar to that in the first DECOVALEX project in 1991-1995 (Eloranta 1996). The group was open to all who were interested in the problematics of the international project.

The members of the NDG have been (the organization and its representative(s) in parentheses)

- VTT Communities and Infrastructure (Lic.Tech. Jukka Põllä, Dr.Tech. Auli Niemi, Lic.Tech. Tiina Vaittinen, M.Sc.(Tech.) Juhani Korkealaakso, M.Sc.(Tech.) Jaakko Vuopio, M.Sc. (Tech.) Tuomas Pantsar),
- Helsinki University of Technology, Laboratory of Rock Engineering (Prof. Pekka Särkkä, Lic. Tech. Harri Kuula),
- Gridpoint Finland Oy (M.Sc.(Tech.) Matti Hakala),
- BBK Rock Design Oy (M.Sc.(Tech.) Mikael Rinne),
- Saanio & Riekkola Consulting Engineers (Lic.Tech. Erik Johansson),
- Posiva Oy (Lic.Tech. Jukka-Pekka Salo),
- STUK (Dr.Tech. Esko Eloranta), Chairman.

The group gathered 13 times during the years 1996–1999.

# 5 SUMMARY

An international co-operative project, called DECOVALEX II, was in operation 1995-1999. The project was set up by the Swedish Nuclear Power Inspectorate (SKI) as a continuation project of DECOVALEX (1991–1995). The main purpose was to acquire more knowledge about the coupled thermo-hydro-mechanical processes interacting in a spent fuel repository.

DECOVALEX II had four Tasks, two of which dealt with the full-scale *in-situ* tests, carried out in Sellafield in UK (Task 1), and Kamaishi Mine in Japan (Task 2), respectively. Two other tasks dealt with the constitutive relationships of rock joints (Task 3) and the coupled thermo-hydro-mechanical issues related to repository design and performance (Task 4).

The Finnish contributions were first concentrated on Task 3 and later on on the subtask 1C of Task 1. Task 4 was a common discussion forum for all participants concerning THM issues in Performance Assessments. The Finnish contribution to Task 4 was restricted to review work.

The DECOVALEX II project has continued as the DECOVALEX III project which will be carried out in 1999–2002. STUK participates also in DECOVALEX III.

# REFERENCES


Eloranta, E. (ed.), 1996. The international DECOVALEX project for the modelling of coupled Thermo-Hydro-Mechanical processes in a nuclear waste repository. The Finnish contribution during 1991–1995. Finnish Centre for Radiation and Nuclear Safety, Report STUK-YTO-TR 113, November 1996.

Jing, L., Stephansson, O., Börgesson, L., Chijimatzu, M., Kautsky, F., and Tsang, C.-F., 1999. DECOVALEX II Project. Technical Report – Task 2C. SKI Report 99:23, May 1999.

Jing, L., Stephansson, O., Knight, L.J., Kautsky, F., and Tsang, C.-F., 1999. DECOVALEX II Project. Technical Report – Task 1C. SKI Report 99:22, May 1999.

Jing, L., Stephansson, O., Tsang, C.-F., Chijimatsu, M., and Kautsky, F., 1998. DECOVALEX II Project. Technical Report – Task 2A and 2B. SKI Report 98:40, August 1998.

Jing, L., Stephansson, O., Tsang, C.-F., Knight, L.J., and Kautsky, F., 1998. DECOVALEX II Project. Technical Report – Task 1A and 1B. SKI Report 98:39, August 1998.

Jing, L., Stephansson, O., Tsang, C.-F., Knight, L.J., and Kautsky, F., 1999. DECOVALEX II Project. Executive Summary. SKI Report 99:24, November 1999.

Kuusela-Lahtinen, A., Kajanen, J., and Pöllä, J., 1996. Preliminary test on flow properties of a single fracture under normal stress. *In*: E. Eloranta (ed.), The international DECOVALEX project for the modelling of coupled Thermo-Hydro-Mechanical processes in a nuclear waste repository. The Finnish contribution during 1991–1995. Finnish Centre for Radiation and Nuclear Safety, Report STUK-YTO-TR 113, pp. 61–75 (Appendix C), November 1996.

Niemi, A. (ed.), 1999. Studies on coupled hydromechanical effects in single fractures. A contribution to DECOVALEX II Task 3 “Constitutive relationships of rock joints”. Radiation and Nuclear Safety Authority, Report STUK-YTO-TR 151, January 1999.

Pöllä, J., Kuusela-Lahtinen, A., and Kajanen, J., 1996. Experimental study on the coupled T-H-M – processes of single rock joint with a triaxial test chamber. *In:* O. Stephansson, L. Jing, and C.-F. Tsang (eds.), Coupled Thermo-Hydro-Mechanical Processes of Fractured Media, Mathematical and Experimental Studies, Recent developments of DECOVALEX project for radioactive waste repositories. Developments in Geotechnical Engineering, vol. 79, pp. 449-465, Elsevier, Amsterdam – Lausanne – New York – Oxford – Shannon – Tokyo.

Stephansson, O., Hudson, J.A., Tsang, C.-F., Jing, L., and Andersson, J., 1999. DECOVALEX II Project. Coupled THM Issues Related to Repository Design and Performance – Task 4. SKI Report 99:7, March 1999.

Vuopio, J. and Pöllä, J., 1997. Characterization of the Rock Joint Surface. A contribution to DECOVALEX II Task 3 “Constitutive relationships of rock joints”. Radiation and Nuclear Safety Authority, Report STUK-YTO-TR 138, 31 p., December 1997.

# Appendix 1

## Task 1C
## Sellafield shaft

### Part I

Derivation of parameters and continuum simulations

Jukka Pöllä

# A1-1 Introduction

The DECOVALEX II project consists of two modelling excercises, which are called TASK 1 and TASK 2. The Task 1 was proposed by Nirex and it deals with the shaft sinking at the Sellafield area in UK. Task 2 was proposed by PNC, Japan, and it deals with heater-bentonite test to be carried out in Kamaishi mine.

The Radiation and Nuclear Safety Authority (STUK) decided to participate in TASK 1. The scope of the TASK 1 is to model the coupled hydromechanical responses in the Borrowdale Volcanic Group (BVG) from shaft excavation (Fig. A1-1). The shaft is part of the rock characterisation facility (RCF). The shaft is sunk on the line of borehole RFC3. The diameter of the shaft is 5.4 m below 431.5 m bOD down to its total depth at 680 bOD. The part of shaft forming modelling excercise lies between 640 m to 680 m bOD. This sector lies generally unfaulted BVG.

The shaft is excavated by drill and blast methos in rounds of 2.5 m. The rate of shaft sinking is 1 round per two days. Grouting will be carried out where the inflow is greater than 25 l/min. The shaft will be lined down to the top of the BVG. In the BVG reinforcement (rock bolts, mesh, shotcrete) will be based on the rock quality met during the excavation process.

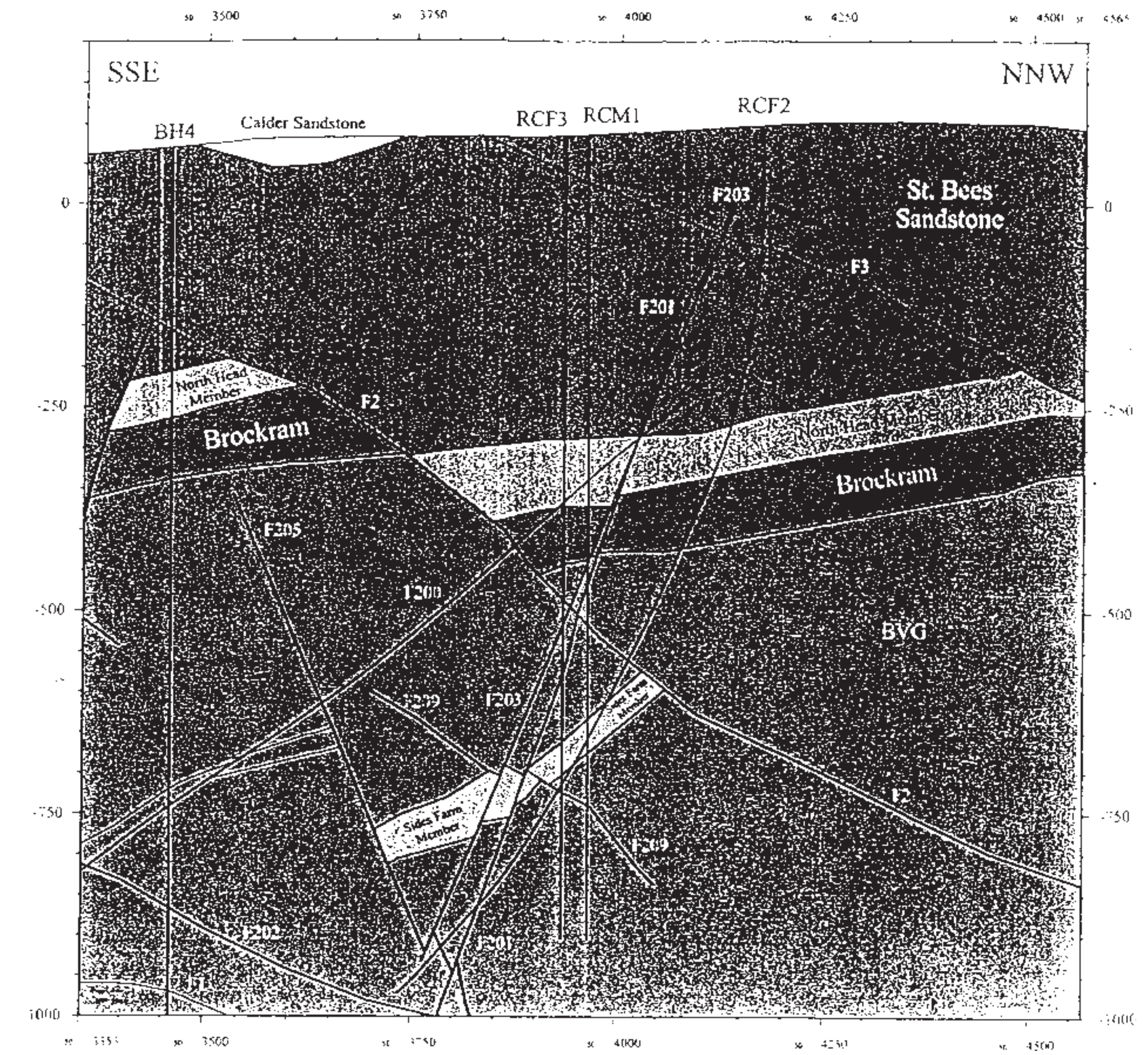


Borehole RCF 2 shown in approximate position

250 m

Dwg. 8805r3 | Date 17/3/97 | Project No.96524800 | Drawn by CW

***Figure A1-1**. SSE–NNW oriented geological cross-section of the Potential Repository Zone.*

# A1-2 Material, discontinuity and rock mass properties

## A1-2.1 Properties given by Nirex

Material and discontinuity properties were given by Nirex. Material properties tested from cores and derived from wireline measurements are shown in Table A1-I. Discontinuity spatial and mechanical properties are shown in Table A1-II. Rock mass properties and rock strength parameters are given in Table A1-III and rock mass hydraulic parameters are given in Table A1-IV.

***Table A1-I.*** *Summary of material properties.*

| | Core data | | | Wireline data | | |
|---|---|---|---|---|---|---|
| Property | **Max.** | **Min.** | **Mean** | **Max.** | **Min.** | **Mean** |
| UCS (MPa) | 308.8 | 29.1 | 157.0 | | | |
| Young's Modulus (GPa) | 97.50 | 73.80 | 84.60 | 99.56 | 31.17 | 69.08 |
| Poisson's Ratio | 0.25 | 0.22 | 0.24 | 0.354 | 0.168 | 0.263 |
| Effective Porosity (%) | 4.53 | 0.05 | 0.86 | | | |
| Porosity (%) | | | | 12.66 | 0.01 | 5.19 |
| Saturated density (Mg/m$^3$) | 2.92 | 2.66 | 2.75 | | | |
| Bulk density (Mg/m$^3$) | | | | 2.82 | 2.58 | 2.69 |
| Hoek-Brown m value | 9.78 | 3.171 | 7.453 | | | |
| Hoek-Brown s value | 1.71 | 0.63 | 1.62 | | | |
| Apparent cohesion of intact rock from triaxial test (MPa) | 56.55 | 11.32 | 30.0 | | | |
| Compressional Sonic Velocity (km/s) | | | | 6.59 | 3.89 | 5.60 |
| Shear Sonic Velocity (km/s) | | | | 3.84 | 2.11 | 3.18 |

***Table A1-II.*** *Discontinuity spatial and mechanical properties.*

| | Set 1 | Set 2 | Set 3 | Set 4 |
|---|---|---|---|---|
| Mean Dir/Dip Dir | 08/145 | 88/148 | 76/021 | 69/087 |
| Max/Min Spacing (m) | 5.35/0 | 2.21/0 | 2.01/0 | 3.54/0 |
| Mean Spacing (m) | 0.29 | 0.26 | 0.28 | 0.31 |
| Residual Friction Angle | 24.9 | 28.0 | 27.0 | 31.0 |
| $JRC_{300}$ | 2.84 | 4.20 | 2.75 | 3.00 |
| $JCS_{300}$ | 61 | 196 | 160 | 220 |

***Table A1-III.*** *Rock mass properties and rock strength parameters (mean values).*

| | |
|---|---|
| NGI Q value | 44.55 |
| RMR value (RMR =12log$_{10}$(Q)+52) | 71.79 |
| Hoek-Brown m value | 6.21 |
| Hoek-Brown s value (undisturbed rock mass) | 0.04 |
| Interpreted $E_{mass}$ (GPa) | 65.00 |

***Table A1-IV.*** *Rock mass hydraulic parameters.*

| | |
|---|---|
| N | 5 |
| Mean log$_{10}$k | –9.03 |
| Min | –10.92 |
| Max | –6.69 |

***Table A1-V.*** *The in-situ state of stress at depths 640 bOD, 660 bOD and 680 bOD.*

| In-situ state of stress | 640 bOD D = 725 m | 660 bOD D = 745 m | 680 bOD D = 765 m | 640 bOD mean | 660 bOD mean | 680 bOD mean |
|---|---|---|---|---|---|---|
| $\sigma_{v\ max}$ (MPa) | 18.78 | 19.29 | 19.79 | $\sigma_v$ =18.35 | $\sigma_v$ =18.85 | $\sigma_v$ =19.35 |
| $\sigma_{v\ min}$ (MPa) | 17.91 | 18.41 | 18.90 | | | |
| $\sigma_{Hmin\ (max)}$ (MPa) | 16.13 | 16.55 | 16.97 | $\sigma_{Hmin}$ =14.15 | $\sigma_{Hmin}$=14.55 | $\sigma_{Hmin}$ =14.95 |
| $\sigma_{Hmin\ (min)}$ (MPa) | 12.18 | 12.56 | 12.93 | | | |
| $\sigma_{Hmax\ (max)}$ (MPa) | 25.55 | 29.05 | 29.72 | $\sigma_{Hmax}$ =23.04 | $\sigma_{Hmax}$ =25.08 | $\sigma_{Hmax}$ =25.70 |
| $\sigma_{Hmax\ (min)}$ (MPa) | 20.53 | 21.10 | 21.68 | | | |

## A1-2.2 Derived parameters for modelling

### A1-2.2.1 The state of stress

The in-situ state of stress is governed by the following equations:

$\sigma_v$ = (0.02494 ± 0.00025)D + (0.26622 ± 0.25326) MPa

$\sigma_{Hmin}$ = (0.01996 ± 0.00113)D – (0.31619 ± 1.15545)MPa

$\sigma_{Hmax}$ = (0.03113 ± 0.00227)D + (1.88747 ± 2.284202)MPa

where D = depth in m $bGL_{TVD}$. The $bGL_{TVD}$ is 85 m above bOD.

The orientation of $\sigma_{Hmax}$ is 340º from north.

The in-situ state of stress at depths 640 bOD, 660 bOD and 680 bOD calculated according to equations above are shown in Table A1-V.

The vertical stress induced by gravity at the depth of 660 bOD is 19.7 MPa, which is close to the calculated mean vertical stress.

***Table A1-VI.*** *Normal stiffnesses according to laboratory tests.*

| RFC1 $k_n$ (GPa/m) | RFC2 $k_n$ (GPa/m) | RFC3 $k_n$ (GPa/m) |
|---|---|---|
| 5.73 | 7.35 | 7.91 |
| 7.61 | 5.9 | 5.72 |
| 3.66 | 8.47 | 4.81 |
| 5.72 | 6.79 | |
| 5.68 | | |
| 8.06 | | |
| 5.25 | | |
| 7.63 | | |
| **mean 6.17** | **mean 7.13** | **mean 6.15** |

### A1-2.2.2 Normal stiffness

According to the test results provided by Nirex, the normal stiffnesses of joints are according to the Table A1-VI. The normal stresses used in the tests have been about 1 MPa.

The normal stiffness is highly stress-dependent. The in-situ stresses are higher than stresses

***Table A1-VII.*** *Shear stiffnessess of the tested joints.*

| Sample | τ (MPa) | s (mm) | $k_s$ (MPa/mm) | Average |
|---|---|---|---|---|
| 1-226 | 1.1 | 0.4 | 2.75 | |
| 1-227 | 0.6 | 0.3 | 2.00 | |
| 1-228 | 1 | 0.75 | 1.33 | |
| 1-229 | 1 | 0.4 | 2.50 | |
| 1-231 | 0.6 | 0.4 | 1.50 | |
| 1-230 | 1 | 0.65 | 1.54 | 1.94 |
| 2-185 | 0.8 | 0.3 | 2.67 | |
| 2-183 | 0.4 | 0.25 | 1.60 | |
| 2-182 | 0.6 | 0.9 | 0.67 | |
| 2-180 | 0.9 | 0.9 | 1.00 | 1.48 |
| 3-441 | 1.6 | 0.95 | 1.68 | |
| 3-442 | 0.4 | 0.3 | 1.33 | |
| 3-444 | 0.8 | 0.5 | 1.60 | 1.54 |
| **Average** | | | **1.71** | |

used in laboratory tests and thus the in-situ normal stiffnesses are also higher.

The normal stiffness $k_n$ and normal stress $\sigma_n$ is related according to equation

$$\frac{\sigma_n^2}{k_n} = \xi V_{mc}$$

where $\xi$ is seating pressure and $V_{mc}$ is maximum possible joint closure.

Computing $\xi V_{mc}$ from the test results gives the average $k_n$ = 2570 GPa/m, when the normal stress is 20 MPa.

### A1-2.2.3 Shear stiffness

Shear stiffnesses calculated from laboratory tests are shown in Table A1-VII.

Empirical relation between shear stiffness and normal stress is (Barton Choubey, 1977)

$$k_s = \frac{100}{L}\sigma_n \tan\left[JRC\log_{10}\left(\frac{JCS}{\sigma_n}\right)+\varphi_r\right]$$

When normal stress is 20 MPa, equation gives $k_s$ = 3,9 GPa/m (JRC=3.2, JCS = 160 MPa, $\varphi_r$ = 27.7°).

### A1-2.2.4 Elastic constants

Bulk modulus $K_{jointed}$ and shear modulus $G_{jointed}$ for randomly jointed rock mass can be calculated according to Fossum (1985)

$$K_{jointed} = \frac{1}{9}E\left[\frac{3(1+\upsilon)sk_n + 2E}{(1+\upsilon)[1-2\upsilon]sk_n + (1-\upsilon)E}\right]$$

$$G_{jointed} = \frac{1}{30}\left[\frac{E}{(1+\upsilon)}\frac{9(1+\upsilon)(1-2\upsilon)sk_n + (7-5\upsilon)E}{(1+\upsilon)(1-2\upsilon)sk_n + (1-\upsilon)E}\right] + \frac{2}{5}\frac{Esk_s}{2(1+\upsilon)sk_s + E}$$

$$\nu_{jointed} = \frac{3K_{jointed} - 2G_{jointed}}{2(3K_{jointed} + G_{jointed})}$$

where

E is Young's modulus for intact rock
ν is Poisson ratio for intact rock
s is joint spacing
$k_n$, $k_s$ is joint normal and shear stiffness.

When values given in previous sections are applied, the bulk modulus $K_{jointed}$ is 52.7 GPa and $G_{jointed}$ is 20.4 GPa.

# A1-3 Analytical solutions

If elastic state is assumed, the horizontal tangential stress $\sigma_t$ and radial stress $\sigma_r$ can be calculated according to Kirsch formulae (Brady & Brown, 1985)

$$\sigma_t = \frac{\sigma_{H\max}}{2}\left[\begin{array}{l}(1+K)\left(1+\frac{a^2}{r^2}\right)\\ +(1-K)\left(1+\frac{3a^4}{r^4}\right)\cos 2\theta\end{array}\right]$$

$$\sigma_r = \frac{\sigma_{H\max}}{2}\left[\begin{array}{l}(1+K)\left(1-\frac{a^2}{r^2}\right)-\\ (1-K)\left(1-4\frac{a^2}{r^2}+\frac{3a^4}{r^4}\right)\cos 2\theta\end{array}\right]$$

where $K = \sigma_{Hmax}/\sigma_{Hmin}$, a is a radius of the shaft and r is the distance from the centerpoint of the shaft and θ is the angle measured counterclockwise from the direction of $\sigma_{Hmin}$ (Fig. A1-2).

Tangential displacements $u_t$ and radial displacements are

$$u_t = -\frac{\sigma_{H\max}a^2}{4Gr}\left[\begin{array}{l}(1+K)\\ -(1-K)\left\{2(1-2\upsilon)+\frac{a^2}{r}\right\}\cos 2\theta\end{array}\right]$$

$$u_r = -\frac{\sigma_{H\max}a^2}{4Gr}\left[(1-K)\left\{2(1-2\upsilon)+\frac{a^2}{r}\right\}\sin 2\theta\right]$$

At the level 660 m, state of in-situ stress is: $\sigma_v = 18.85$ MPa, $\sigma_{Hmin} = 14.55$ MPa and $\sigma_{Hmax} = 25.08$ MPa

When derived parameters are applied to the equations above, calculated stresses and displacement at the level 660 m bOD are:

*Total tangential stress (MPa):*

| Distance | 0*D | 0.5D | 1.0D | 2.0D |
|---|---|---|---|---|
| Diagonal 1 | 61.0 | 36.9 | 30.9 | 26.3 |
| Diagonal 2 | 17.0 | 19.4 | 17.8 | 15.2 |

*Tangential stress change (MPa):*

| Distance | 0*D | 0.5D | 1.0D | 2.0D |
|---|---|---|---|---|
| Diagonal 1 | 35.9 | 11.8 | 5.8 | 1.2 |
| Diagonal 2 | 2.5 | 4.9 | 3.3 | 0.7 |

*Radial stress (MPa):*

| Distance | 0*D | 0.5D | 1.0D | 2.0D |
|---|---|---|---|---|
| Diagonal 1 | 0 | 11.6 | 13.6 | 14.1 |
| Diagonal 2 | 0 | 9.8 | 15.6 | 22.5 |

*Radial stress change (MPa):*

| Distance | 0*D | 0.5D | 1.0D | 2.0D |
|---|---|---|---|---|
| Diagonal 1 | -14.5 | -2.6 | -0.9 | -0.4 |
| Diagonal 2 | -25.1 | -15.3 | -9.5 | -2.6 |

*Displacements (mm):*

| Distance | 0*D | 0.5D | 1.0D | 2.0D |
|---|---|---|---|---|
| Diagonal 1 | -0.68 | -0.59 | -0.33 | -0.21 |
| Diagonal 2 | -1.90 | -1.13 | -0.53 | -0.31 |

where D is a shaft diameter and distance is shaft diameters outwards from the shaft wall.

Convergence of shaft along:
Diagonal 1 1.36 mm
Diagonal 2 3.8 mm.

***FLAC3D 2.00*** Job Title: sellafield m-c continuum Technical research Centre of Finland VTT

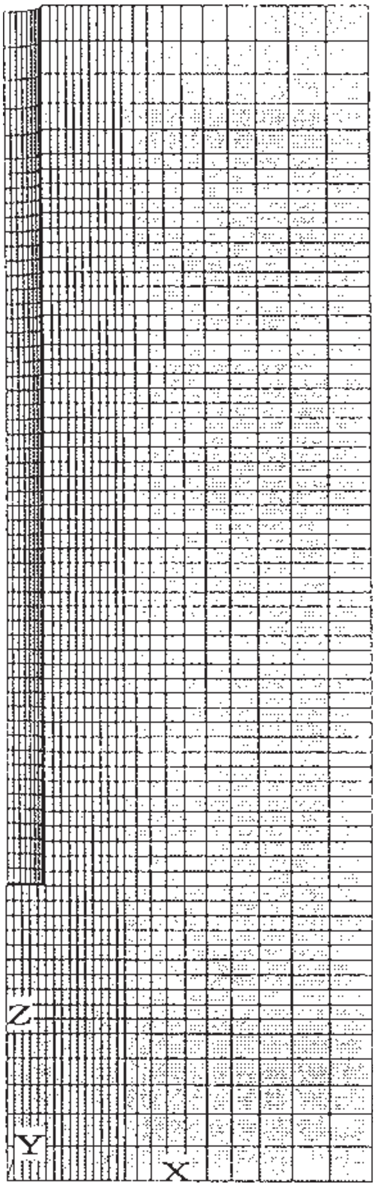


Step 8490 Model Perspective
09:15:50 Mon Jun 29 1998
Center: Rotation:
X: 1.250e+001 X: 0.000
Y: 1.250e+001 Y: 0.000
Z: 4.000e+001 Z: 0.000
Dist: 2.337e+002 Mag.: 1
Ang.: 22.500
Surface
Axes
Linestyle ————————

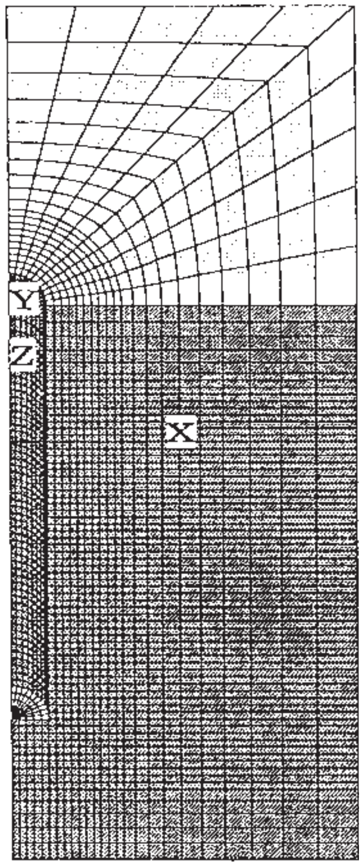


Step 8490 Model Projection
09:40:13 Mon Jun 29 1998
Center: Rotation:
X: 1.250e+001 X: 60.000
Y: 1.250e+001 Y: 0.000
Z: 4.000e+001 Z: 0.000
Dist: 2.337e+002 Size: 9.297e+001

Surface
Axes
Pos: (0.000000e+000, 0.000000e+000)
Linestyle ————————

***Figure A1-2. a)*** *Model geometry* ***b)*** *Model geometry showing the upper surface of the model.*

# A1-4 Numerical simulation

## A1-4.1 Continuum model

In continuum model code FLAC 3D v.2 is used. One quadrant of the shaft is modelled. The top of the model is at level 620 m bOD and the bottom at the level 700 bOD. The width is 25 m. Number of zones in the model is 17500 and number of grid-points is 19596. The model geometry is shown in Fig. A1-2. The in-situ stress used is according to the Table A1-V. Material parameters are bulk modulus 52.75 GPa, shear modulus 20.4 GPa, cohesion 30 MPa and friction angle 27.7º.

The depth between levels 640–680 is "excavated" in 10 m intervals. Because the rate of shaft sinking is 2.5 m in two days, the time used in 10 m interval is 8 days. The displacements are followed at the level 660 bOD during the "excavation". Stresses are followed in zones adjacent to the points.

D3 is the axis in the direction of $\sigma_{Hmin}$(x) and D1 is the axis in the direction of $\sigma_{Hmax}$(y). Distances from shaft wall are: 1: 0*D; 2: 0.5D; 3: D; 4: 2D, where D is a shaft diameter.

The numbering of the points is shown in Fig. A1-3. The results of the shaft simulation are:

*Time 0 days, bottom at the level 640 m bOD.*

| Point | $\sigma_x$ (MPa) | $\sigma_y$ (MPa) | x -displ. (mm) | y-displ. (mm) |
|---|---|---|---|---|
| D3/1 | 14.5 | 25.1 | 0 | 0 |
| D3/2 | 14.5 | 25.1 | 0 | 0 |
| D3/3 | 14.5 | 25.1 | 0 | 0 |
| D3/4 | 14.5 | 25.1 | 0 | 0 |
| D1/1 | 14.5 | 25.1 | 0 | 0 |
| D1/2 | 14.5 | 25.1 | 0 | 0 |
| D1/3 | 14.5 | 25.1 | 0 | 0 |
| D1/4 | 14.5 | 25.1 | 0 | 0 |

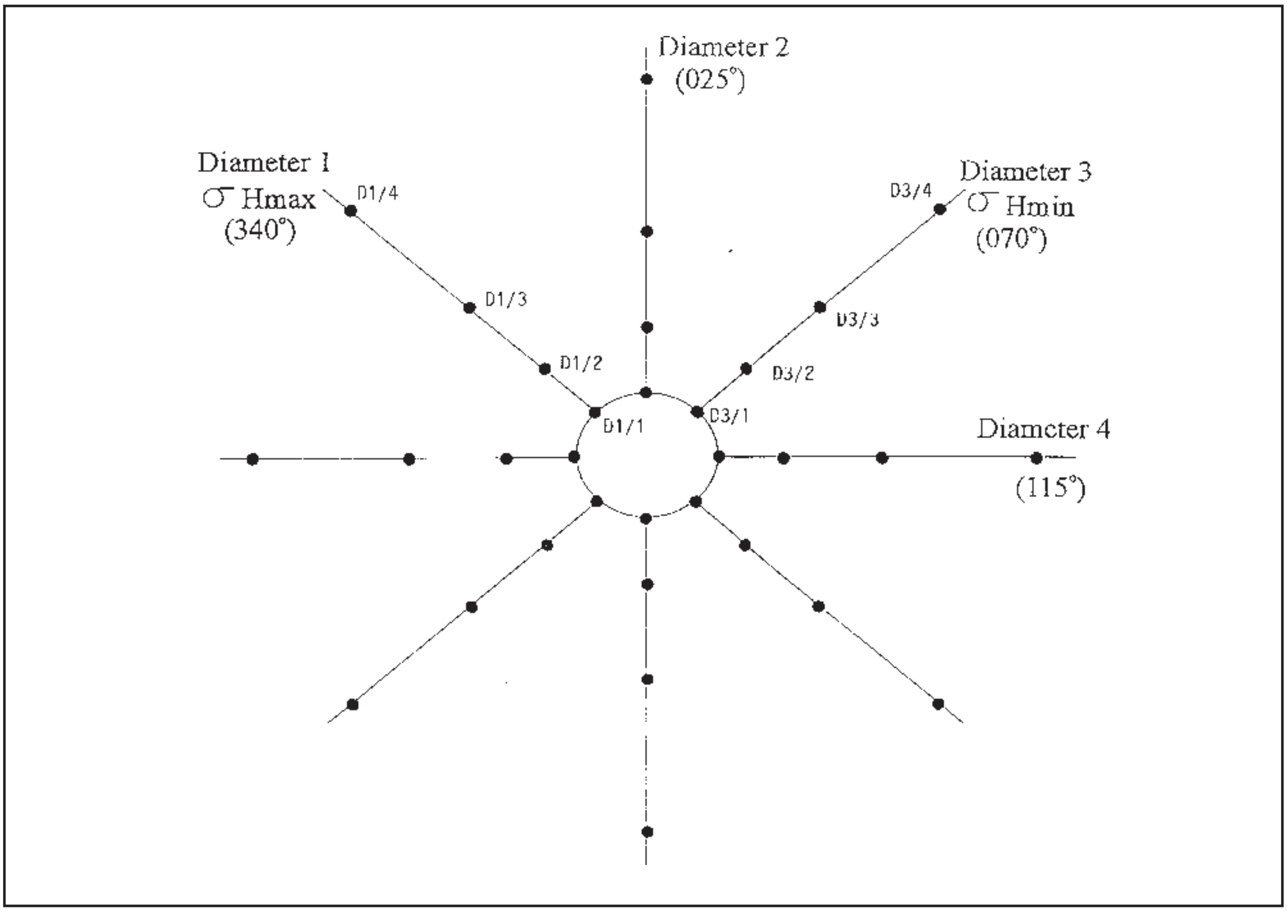


***Figure A1-3.*** *Layout of diagonals and monitoring points.*

**APPENDIX 1**

*Time 8 days, bottom at the level 650 m bOD.*

| Point | $\sigma_x$ (MPa) | $\sigma_y$ (MPa) | x -displ. (mm) | y-displ. (mm) |
|---|---|---|---|---|
| D3/1 | 14.5 | 25.1 | 0 | 0 |
| D3/2 | 14.5 | 25.1 | 0 | 0 |
| D3/3 | 14.5 | 25.1 | 0 | 0 |
| D3/4 | 14.5 | 25.1 | 0 | 0 |
| D1/1 | 14.5 | 25.1 | 0 | 0 |
| D1/2 | 14.5 | 25.1 | 0 | 0 |
| D1/3 | 14.5 | 25.1 | 0 | 0 |
| D1/4 | 14.5 | 25.1 | 0 | 0 |

*Time 16 days, bottom at the level 660 m bOD.*

| Point | $\sigma_x$ (MPa) | $\sigma_y$ (MPa) | x -displ. (mm) | y-displ. (mm) |
|---|---|---|---|---|
| D3/1 | 11.5 | 41.9 | 0.175 | 0 |
| D3/2 | 14.5 | 27.5 | 0.075 | 0 |
| D3/3 | 14.5 | 26.0 | 0.05 | 0 |
| D3/4 | 14.5 | 25.2 | 0.01 | 0 |
| D1/1 | 19.7 | 14.0 | 0 | 0.54 |
| D1/2 | 16.2 | 21.5 | 0 | 0.4 |
| D1/3 | 15.4 | 22.9 | 0 | 0.28 |
| D1/4 | 14.8 | 24.0 | 0 | 0.14 |

The convergence along diameter 1 is 3.9 mm and along diameter D3 1.44 mm.

*Time 24 days, bottom at the level 670 m bOD.*

| Point | $\sigma_x$ (MPa) | $\sigma_y$ (MPa) | x -displ. (mm) | y-displ. (mm) |
|---|---|---|---|---|
| D3/1 | 4.4 | 50.0 | 0.72 | 0 |
| D3/2 | 13.5 | 29.8 | 0.23 | 0 |
| D3/3 | 14.0 | 27.0 | 0.14 | 0 |
| D3/4 | 14.2 | 25.8 | 0.07 | 0 |
| D1/1 | 19.6 | 1.7 | 0 | 1.81 |
| D1/2 | 17.6 | 16.2 | 0 | 0.98 |
| D1/3 | 16.3 | 20.0 | 0 | 0.62 |
| D1/4 | 15.0 | 23.0 | 0 | 0.29 |

*Time 32 days, bottom at the level 680 m bOD.*

| Point | $\sigma_x$ (MPa) | $\sigma_y$ (MPa) | x -displ. (mm) | y-displ. (mm) |
|---|---|---|---|---|
| D3/1 | 4.4 | 50.6 | 0.72 | 0 |
| D3/2 | 13.6 | 30.0 | 0.23 | 0 |
| D3/3 | 14.3 | 27.2 | 0.14 | 0 |
| D3/4 | 14.4 | 25.9 | 0.07 | 0 |
| D1/1 | 19.8 | 1.7 | 0 | 1.85 |
| D1/2 | 17.7 | 16.2 | 0 | 0.99 |
| D1/3 | 16.2 | 20.0 | 0 | 0.64 |
| D1/4 | 15.0 | 23.0 | 0 | 0.30 |

The displacements are shown in Fig. A1-4. Stresses are shown in Figs. A1-5 and A1-6.

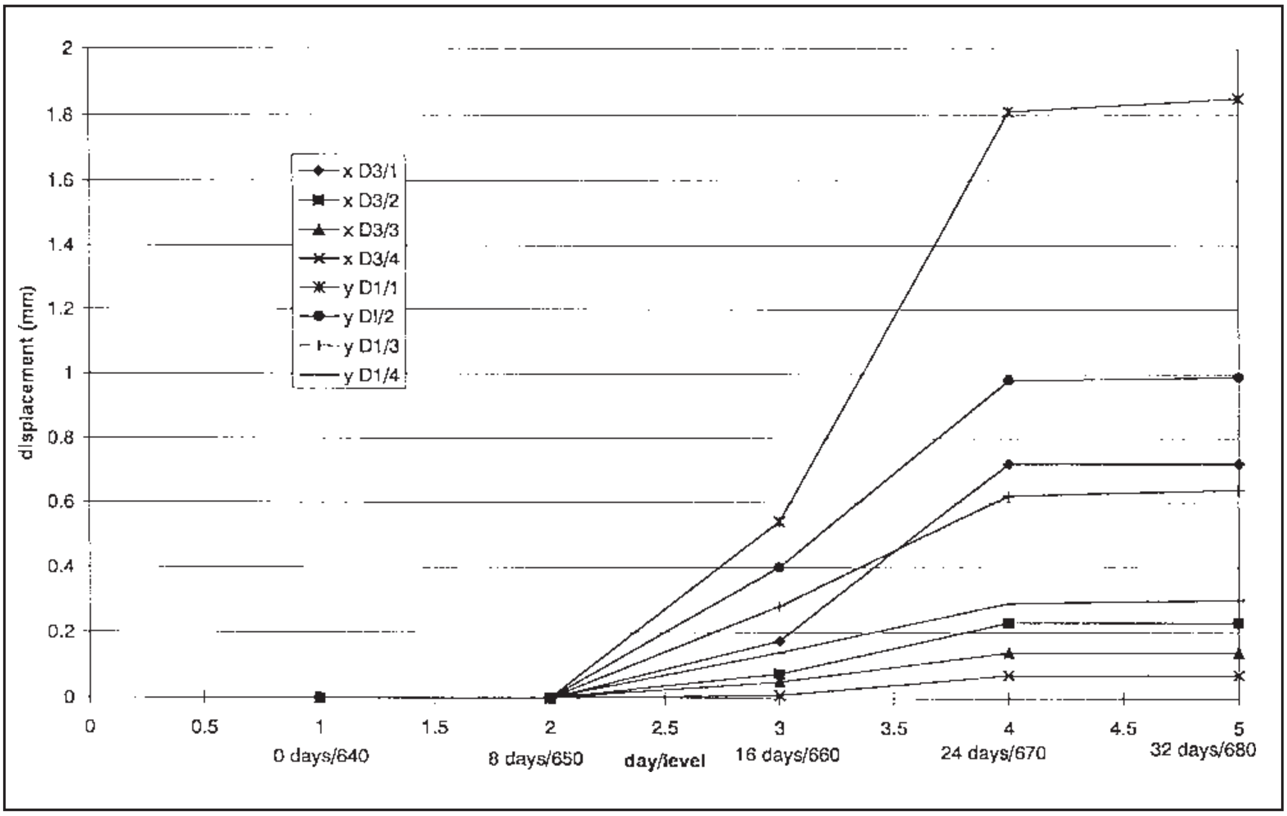


***Figure A1-4.*** *Radial displacements along diameters D1 and D3.*

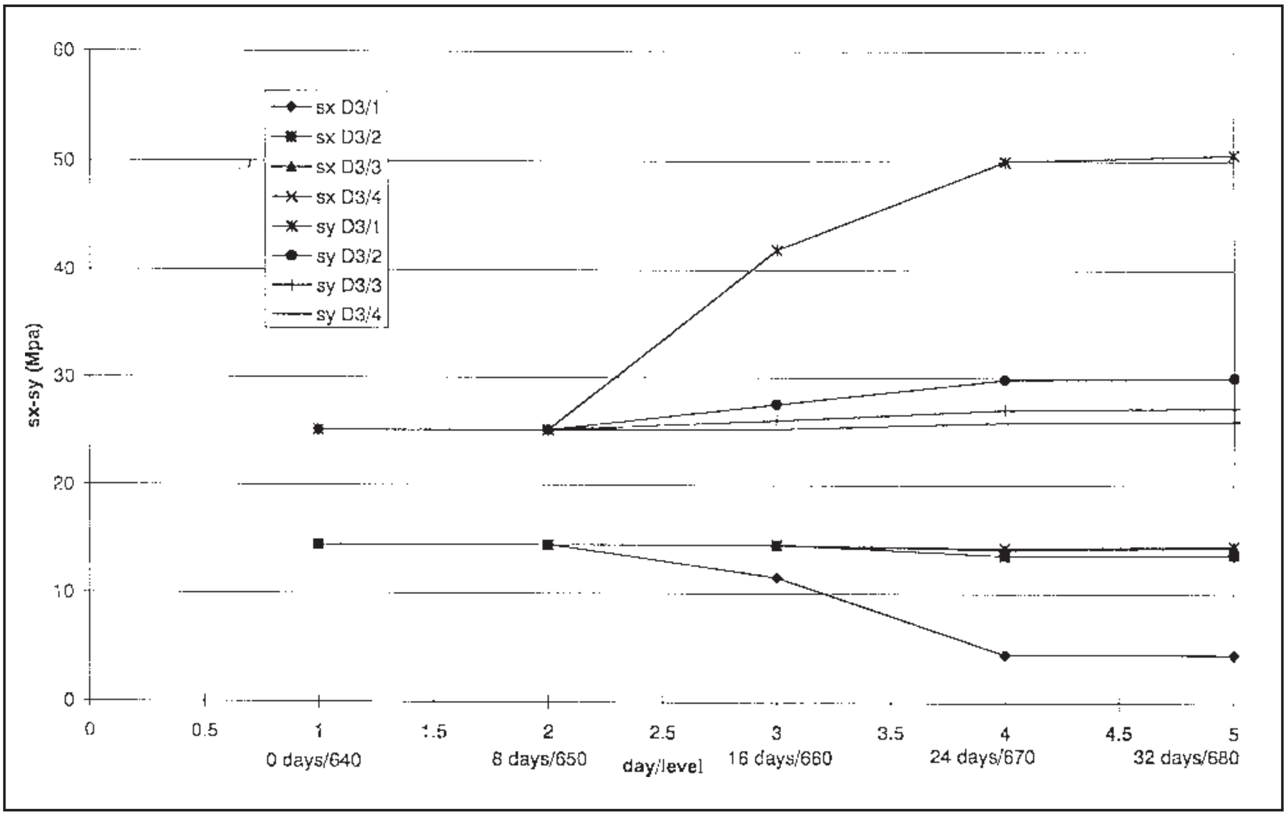


***Figure A1-5.*** *Radial (sx) and tangential (sy) stresses along diameter D3.*

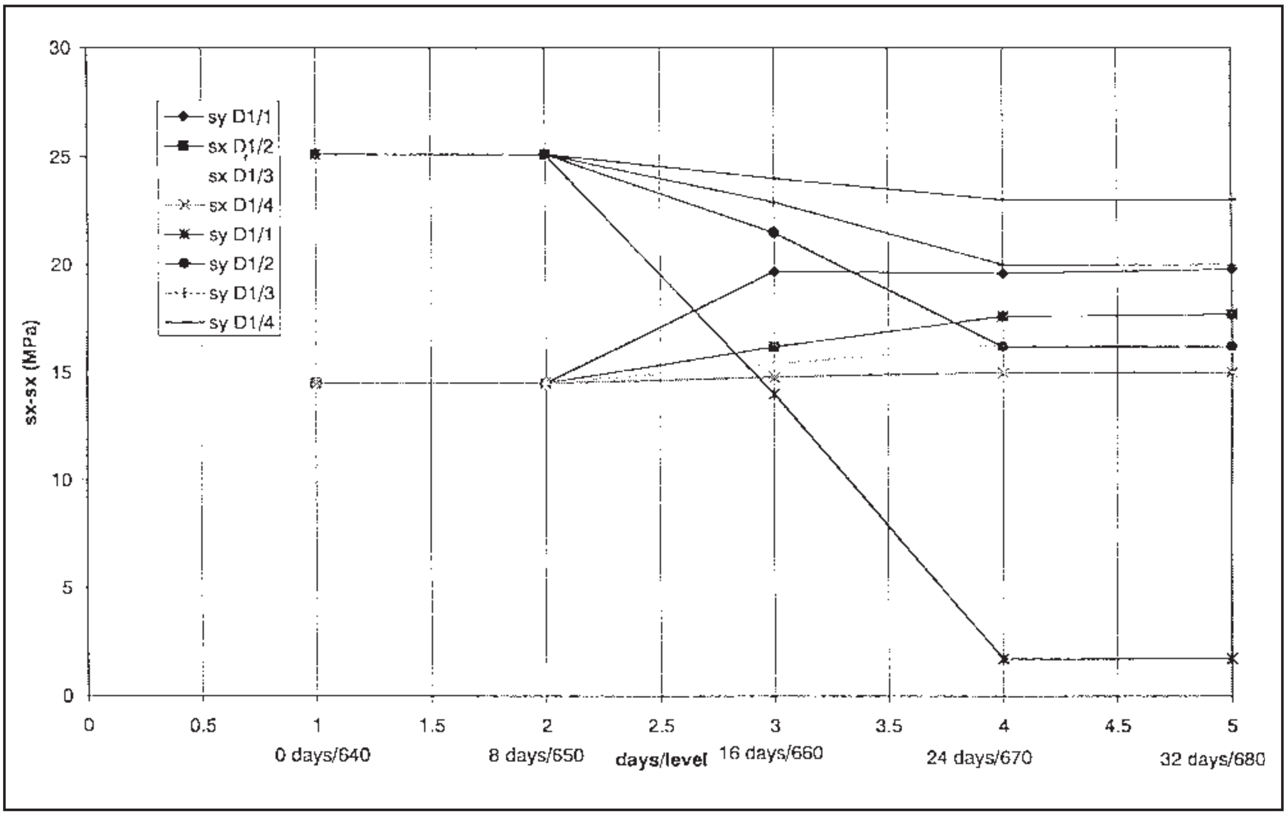


***Figure A1-6.*** *Radial (sy) and tangential (sx) stresses along diameter D1.*

# A1-5 Discussion

Continuum analysis indicates that the convergence of the shaft at 660 m bOD only a few millimeters. One third of the final displacements take place when the shaft bottom is at the monitoring level and two thirds after shaft has passed that level.

It also shows that the influence of the shaft bottom is limited to the range of less than 10 m along the axis of the shaft. When excavation is at the level of 650 m bOD no changes can be seen in the monitoring points at the level of 660 m bOD. Also, when shaft bottom is at the level of 670 m bOD, no changes take place at the 660 m bOD level. A shorter “excavation interval” in the simulation would give more accurate estimate on the extent of the high stress zone in the vicinity of the shaft bottom.

There are no major faults intersecting the simulated zone. These faults may cause local effects which may have some significance in rock reinforcement procedures and grouting measures. These faults should be considered when rock mechanical stability of the shaft is considered. Also, stress changes and displacements within faults may have great influence on the water inflow.

The estimate on the extent of the excavation disturbed zone around the shaft would require analysis which can handle, at least, the growth of existing cracks and criteria for the generation of new cracks.

# A1-6 References

Barton N., Choubey V.1977. The shear strength of rock joints in theory and practice. Rock Mechanics 10.

Brady B.H.G. & Brown E.T.1985. Rock Mechanics for Underground Mining. Chapman & Hall, London.

Fossum A.1985. Effective elastic properties for a randomly jointed rock mass. Int. J. Rock Mech. Min. Sci. & Geomech. Abstr. Vol. 22(6).

Halonen O. 1989. Stability calculations in jointed rock mass. VTT Publications 57. Espoo.

# Appendix 2

## Task 1C
## Sellafield shaft

### Part II

VTT flow prediction

Juhani Korkealaakso, Jaakko Vuopio, Tuomas Pantsar

**APPENDIX 2** PART II: VTT FLOW PREDICTION

# A2-1 Introduction

The DECOVALEX II project consists of two modelling exercises called TASK1 and TASK2. The TASK 1 was proposed by Nirex and it deals with the shaft sinking at the Sellafield area in UK. TASK 2 was proposed by PNC, Japan, and it deals with heater-bentonite test to be carried out in Kamaishi.

The Radiation and Nuclear Safety Authority (STUK) decided to participate in TASK 1. The scope of the TASK 1 is to model the coupled hydromechanical responses in the Borrowdale Volcanic Group (BVG) from shaft excavation. The shaft will be part of the rock characterization facility (RCF). The shaft will be sunk on the line of borehole RFC3. The diameter of the shaft is 5.4 m and it will be located 431.5 m bOD down to its total depth at 680 bOD (below Ordinance datum- mean sea level). The part of shaft, to where the modelling exercises are carried out, lies between 640 m to 680 m bOD.

The primary purpose of the present study is to summarize the predictions, the approach and methods applied by Technical Research Centre of Finland (VTT) to the hydraulic problems of TASK 1C, but it includes also the description and results of preceding hydrogeological conceptualization as well as the calibration processes that were essential to these predictions.

The predictive hydraulic measures of TASK 1C are following

- magnitude of water inflow to section 640-680 m bOD within sector 7 of shaft
- pressure response in adjacent boreholes RCM1 and RCM2 at depths 640 m and 680 m bOD.

# A2-2 TRINET: Numerical simulation of flow and head distributions

The three-dimensional flow and advection-dispersion code, TRINET (Karasaki, 1987; Segan and Karasaki, 1992), and the network generator TRINP3D (Korkealaakso and Kontio, 1995) have been applied in the flow analysis and integration of head distributions, open borehole effects and natural tracer information in the volume between the boreholes. The code is designed to calculate flow and tracer transport on any two- or three-dimensional network of one-dimensional elements. Simulation of flow and transport can be produced in discretely fractured or equivalent continuum aquifers, or in any combination of discrete and continuum aquifers (Karasaki 1986; 1987; 1988. Segan and Karasaki 1993). For example, the code can simulate separate fracture zones as continuum layers which are in turn connected by several discrete fractures. As further work/analysis is carried out at the site and new information and insights are gained, the model can be continually up-dated to accomodate new complexities. When the nodes and elements are distributed on a Cartesian grid with uniform spacing in both dimensions, the model effectively simulates an equivalent porous medium. When the spacing between nodes is sufficiently small, radial flow can be simulated with a high degree of accuracy even over small intervals and close to the pumped well. All of the options for simulating boundary conditions can also be used within the problem domain to simulate sources or sinks of water or internal boundaries.

Hydraulic heads are calculated at all nodes connected by linear, one-dimensional elements, Fig. A2-1. Mathematically, an element represents a finite-dimension rectangular rod of porous material with a particular hydraulic conductivity and specific storage, but is not necessarily meant to represent precisely a specific channel. It may represent the equivalent conductance of several channels combined. Nodes and line elements can be distributed in one-, two-, or three-dimensional space, and each node is connected to at least one line element. The lattice of elements need not be uniformly spaced. It can be two- or three-dimensional, and rectangular, triangular, or a combination of these. The code solves the head distribution over the entire domain using a Galerkin finite element formulation for spatial discretization, and the time derivative is approximated using a finite difference scheme. For the purpose of calculating flow, only the location of the endpoints and the conductance and specific storativity of each element need be known. The conductance has the units of hydraulic conductivity (m/s) times the cross-sectional area (bxw; height times aperture): $m^3/s$ (in the following simulations height of each element b is taken to be one) and the unit is that of transmissivity. For flow calculations it is not necessary to describe the actual shape of the conductor. The flow equation between the two nodes at either end of a one-dimensional finite element may be written

$$S\,\partial h/\partial t = T\,\partial^2 h/\partial x^2 \qquad \text{(A2-1)}$$

where h is the hydraulic head and S and T are the storativity and transmissivity, respectively, of the element.

For a lattice with variable spacing to behave as a uniform porous medium, element properties must vary with lattice spacing. The typical variable lattice used in our simulations has a nested structure. The finest regions with spacing L are around the wells and are surrounded by a central

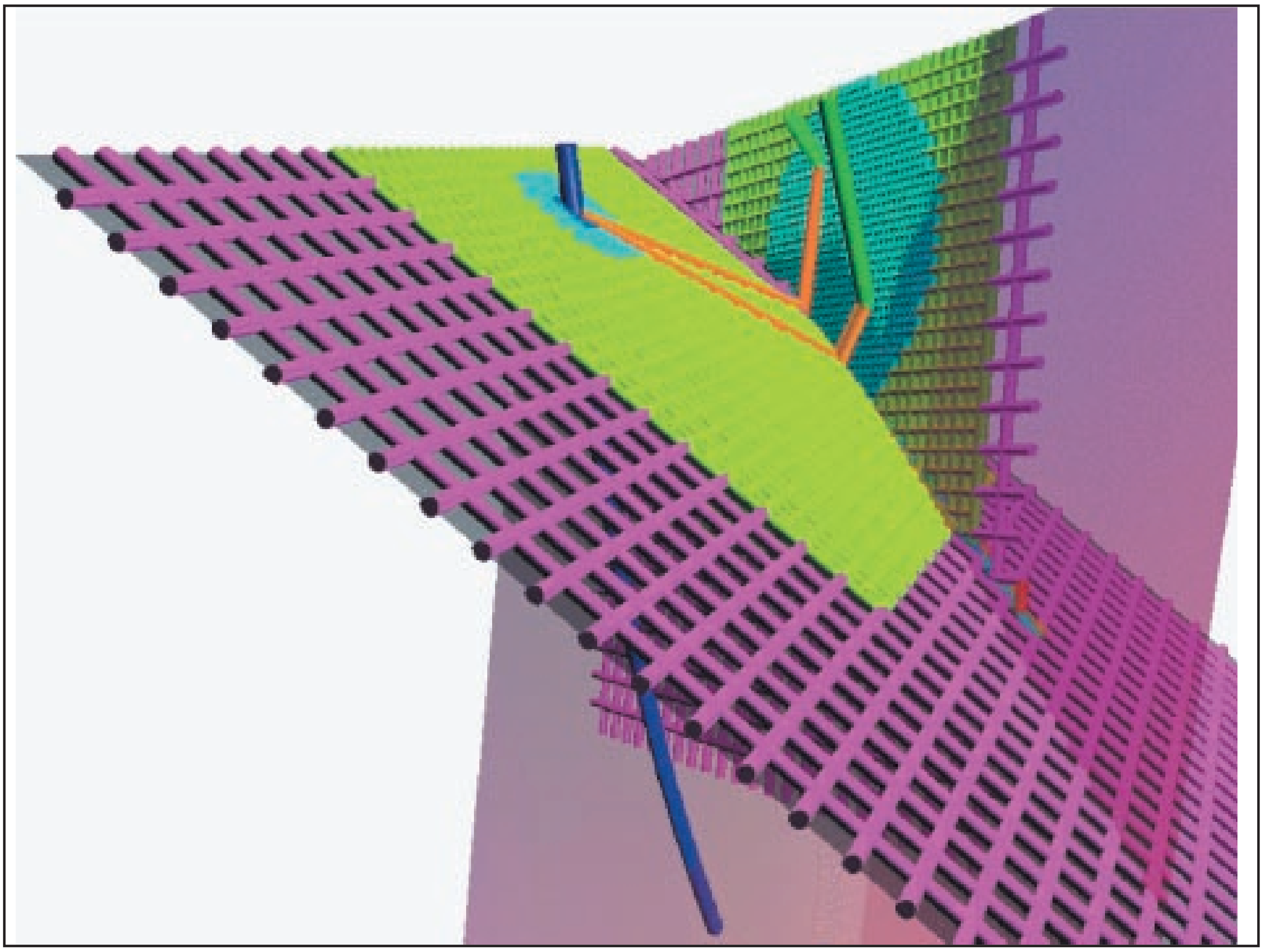

***Figure A2-1.*** *The lattice of one dimensional line elements which intersect the boreholes.*

region with spacing aL, which in turn may be surrounded by a region with spacing $a^2L$. If the lattice spacing increases from L to $a^j$ L, the element properties in our simulations are modified as follows $T \rightarrow a^j$ T and $S \rightarrow a^j$ S.

Doughty (1995) has presented the equations to transform the input parameters of TRINET to the corresponding porous medium equivalents.

TRINET in its standard form (that is only applied in this study) does not account for the possible fluid or solute exchange between the fractures and the porous media, but recently, Birkholzer and Karasaki (1995) have combined and extended the fracture network simulator with a sophisticated method to account for fracture-matrix interaction (TRIPOLY: programs for simulating flow and solute transport in fracture networks embedded in porous matrix blocks). Fractures and matrix blocks are treated as two different systems, and the interaction is modeled by introducing sink/source terms in both systems. It is further assumed that flow and transport in the matrix can be approximated as one-dimensional processes, perpendicular to the adjacent fracture surfaces. The fracture-matrix interaction module allows for detailed studies of spreading processes in fractured porous rock. Since no two- or even three-dimensional discretization of the matrix is needed, a remarkable saving of computer time and storage is achieved compared to hybrid models for fractures and rock.

In the original fracture network version TRINET also creates new nodes only along existing channels and assumes complete mixing at intersections of channels. The code TRIPOR (Ijiri and Karasaki 1994) is an extension of TRINET and can handle also the solute transport in a two-dimensional continuous medium. The special advantage of TRIPOR is in its capability to create new nodes anywhere in a two-dimensional domain while TRINET creates new nodes only along existing channels.

# A2-3 Hydrogeological conceptual model

Based on geological and hydrogeological information prepared and distributed by Nirex (Science report, 1995), a hydrogeological conceptual model of the rock at Sellafield has been constructed. This zone model is considered to contain all the likely major water-conducting pathways which form the basis for the fluid flow calculations. A three-dimensional flow model was then created as two-dimensional lattices of one-dimensional conductors which lie on planes corresponding to the zones given in Figure A2-2.

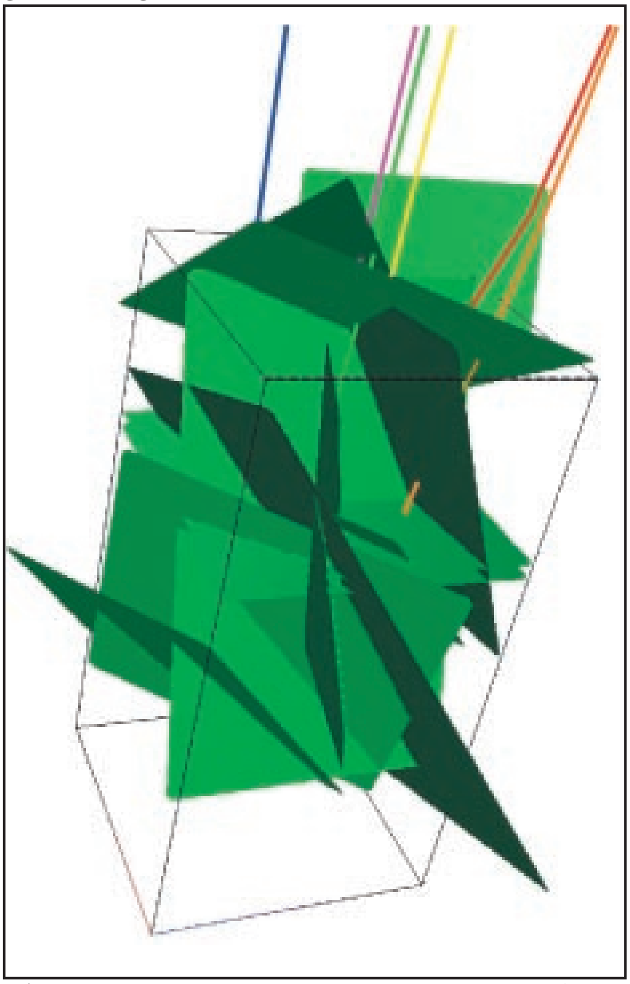

***Figure A2-2.*** *Geometry, boreholes and major faults in the VTT model.*

The boreholes in the zone model intersect the structures at single points. In all boreholes each zone is contained at least in one packed-off interval, which means that the data obtained from the interval are consistent with the model.

The scale of analysis is constrained by the density of the head monitoring points. The minimum spacing of the conductors should be less than that of the monitoring points. It is advantagous to have more than a single element between any two monitoring points to reconstruct the hydraulic head distribution of the fracture zone. In the case of Sellafield, the average spacing of monitoring points is on the order of a few to several tens of metres; a 7 metre grid spacing on each structure zone was selected. To insure a hydraulic connection between the zones and the borehole (if the borehole doesn't intersect any channel in the zones) small "fins" have been added to the boreholes at the points where they intersect the zones.

The purpose of these modelled simulations is to describe the equivalent hydrologic properties of the structural unit rather than individual fractures. The scale of the structures, therefore, is estimated to be on the order of several tens of metres to over a hundred metres in thickness.

In the BVG (Borrowdale Volcanic Group), fracture flow is the dominant mechanism. Previos GIT studies has shown that a lateral variability in the geology and discontinuities are possible pathways for groundwater flow.

The model region was chosen within the BVG since there has been no indications of the flow exchange between BVG and overlying St Bees Sandstone, where the matrix flow has been observed to be the dominant mechanism. The VTT model is based on an assumption that the flow in the BVG is dominated by large scale faults and flow zones.

This VTT 3D-model includes twelve major faults; F2 (both upper and lower), F200, F201, F202, F203, F205, F209, F210, F212, F99U and F99L, chosen by their locations and sizes. Faults are mainly those interpreted by Nirex, but the last two, F99U and F99L, are included to present equivalently the flow system in a productive relatively lower quality rock in the Side Farm Member (SFM). The pump test is connected to the SFM and the two horisontal flow zones connect the source and the monitoring zones to overall flow system. All faults are represented as planar rectangular planes of constant hydraulic transmissivity and storativity. In the final calibrated hydrogeological model the hydrological parameters vary with depth and the structural domain and domain boundaries in the BVG (Figure A2-3).

The dimensions of the model are about 400 m x 400 m × 800 m, located between 400 m and 1200 m bOD. The borehole RCF3 and the source zone P3 (640–680 bOD) are both located approximately in the centre of the model. The other 17 monitoring zones in six additional nearby boreholes (RFC1, RCF2, RCM1, RCM2, RCM3) are connected to the intersections of the modelled faults and boreholes.

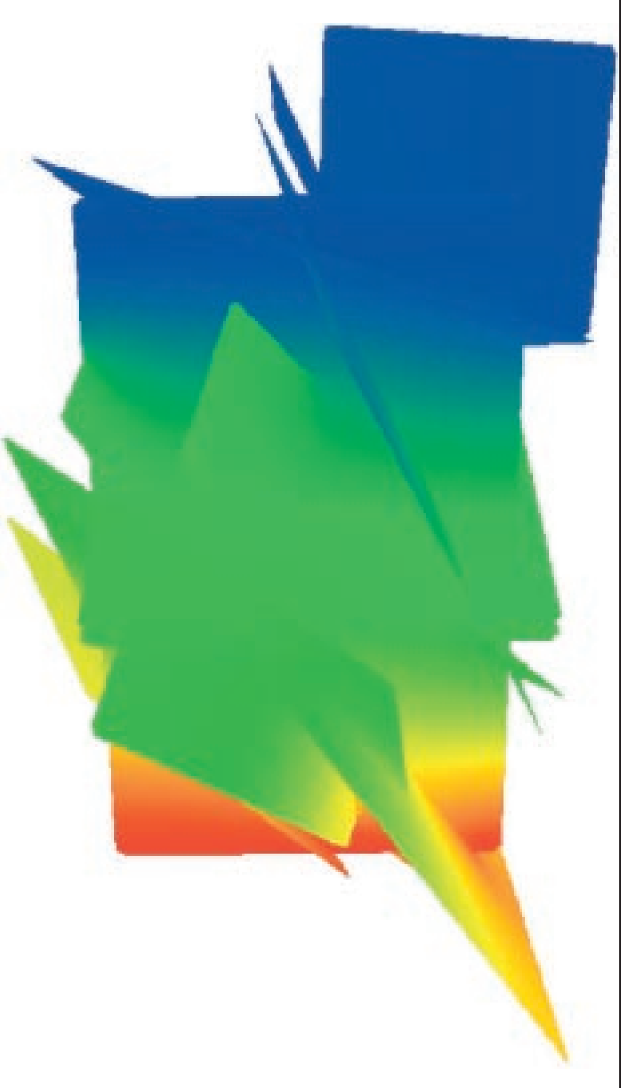

***Figure A2-3.*** *Interpolated 3D head distribution. Head values of the zones decrease with depth by colours from blue to red.*

In the flow and pumping simulations we have based/calibrated our choice of outer boundary conditions on head observations in the boreholes (initial pressures in the monitoring zones provided by Nirex). We feel that these boundary conditions do represent a degree of approximation consistent with the rest of the assumptions we have made in the pumping test and flow simulations. In the RFC3 pumping test simulations constant head boundary conditions have been applied directly to the both ends of the zone F203 (zone is the dominant pathway of flow and controls throughout the whole model). During the predictive calculations of shaft flow the effects of opening the shaft to atmospheric pressure are also included into the model. All the other boundaries are no flow boundaries and there is not any interior boundaries.

## A2-4 Simulation of the RCF3 Pumping Test and Calibration of Material Properties

In this study the model is just calibrated by adjusting conductances and storativities to meet the drawdown and flow conditions due to the RCF3 pumptest. The present calibration is based only on a trial and error approach and conductance and storativity are assumed to be constant and isotropic within each domain (i.e. same material values were assigned to entire single hydraulic conductor domain/zone, included in the model as a deterministic feature) and can therefore be described by a single parameter value. The rationale for having constant values is that it is generally not possible to determine the variability within a hydraulic conductor domain with the techniques used. First of all the evaluated hydraulic properties are derived either from the single interference test responses and represent effective values within a large inluence radius (middle to late time responses) or from the relative differences in single hole test results.

In the calibration process we used trial and error approach to meet measured pressure and flow conditions of the RCF3 pumping test. In our final calibration we used different transmissivity and storativity values in the parallel zones F99U and F99L than in the other zones in the model, Table A2-I.

Calibrated transmissivity ($T_{cal}$):
- 8E-8 (F99U and F99L in BVG)
- 1E-7 (F2, F200, F201, F202, F203, F205, F209, F210, F212)

Calibrated storativity ($S_{cal}$):
- 1E-5 (F99U and F99L in BVG)
- 5E-7 (F2, F200, F201, F202, F203, F205, F209, F210, F212)

PART II: VTT FLOW PREDICTION **APPENDIX 2**

***Table A2-I.*** *Template specifications for the first try and calibrated VTT 3D zone model. Measured (NIREX) and predicted/calibrated pressures in monitoring zones with different transmissivity (T) and storativity (S). Flowrate is calculated at time t=2110h. The calibrated pressures and flowrate are presented in bold and calibrated hydraulic parameters are respectively $T_{cal}$ and $S_{cal}$.*

| **Borehole** | **Depth (m bOD)** | **Drawdown (kPa) at the end of the pumping test (t=2110 h)** | | | | | |
|---|---|---|---|---|---|---|---|
| | | Measured | **Calibrated** | $S=S_{cal}$*10 | $S=S_{cal}/10$ | $T=T_{cal}$*10 | $T=T_{cal}/10$ |
| RCM1 | –438.12 | 24.00 | **1.84** | 0.02 | 18.47 | 19.02 | 0.03 |
| RCM1 | –441.14 | 24.00 | **1.99** | 0.03 | 20.46 | 21.06 | 0.04 |
| RCM1 | –452.25 | 24.00 | **2.18** | 0.03 | 22.29 | 22.97 | 0.11 |
| RCF3 | –520.86 | 51.00 | **6.65** | 0.04 | 51.98 | 53.78 | –0.02 |
| RCM3 | –611.24 | 45.00 | **2.69** | 0.03 | 41.24 | 42.68 | 0.10 |
| RCM2 | –626.17 | 55.00 | **36.24** | 0.17 | 166.97 | 173.99 | 0.18 |
| RCM1 | –650.00 | 116.00 | **116.52** | 1.24 | 334.79 | 355.98 | 1.24 |
| RCM2 | –650.00 | 75.00 | **73.15** | 0.23 | 262.37 | 277.28 | 0.19 |
| RCM3 | –650.00 | 47.00 | **0.35** | 0.02 | 55.33 | 57.89 | 0.02 |
| RCM1 | –670.00 | 116.00 | **95.13** | 0.81 | 329.96 | 331.27 | 0.80 |
| RCM2 | –670.00 | 75.00 | **73.38** | 0.19 | 285.25 | 287.79 | 0.16 |
| RCM3 | –670.00 | 49.00 | **0.30** | 0.03 | 59.23 | 60.45 | –0.01 |
| RCF1 | –684.64 | 40.00 | **0.76** | -0.01 | 45.57 | 46.93 | 0.02 |
| RCF2 | –691.05 | 39.00 | **1.34** | 0.05 | 51.57 | 52.94 | –0.11 |
| RCF3 | –722.86 | 13.00 | **12.53** | 0.03 | 108.36 | 110.96 | –0.24 |
| RCM3 | –727.23 | 49.00 | **8.29** | 0.01 | 76.28 | 78.45 | –0.18 |
| RCM1 | –747.38 | 24.00 | **12.22** | 0.03 | 103.96 | 106.52 | –0.31 |
| RCM2 | –760.14 | 45.00 | **12.31** | 0.03 | 99.52 | 102.06 | –0.46 |
| RCF3 | –818.23 | 13.00 | **3.60** | 0.04 | 49.22 | 50.62 | –0.34 |
| RCM3 | –837.20 | 4.00 | **4.48** | 0.01 | 48.69 | 50.11 | –0.28 |
| RCM1 | –845.40 | 6.00 | **3.35** | 0.05 | 46.71 | 48.01 | –0.48 |
| | | | | | | | |
| Flowrate ( l/min ) | | 0.224 | **0.225** | 0.298 | 0.176 | 1.818 | 0.030 |

APPENDIX 2 PART II: VTT FLOW PREDICTION

# A2-5 Flow and Pressure Predictions

The amount of inflow from the zones that intersect the shaft were predicted. The modelling approach is based on the assumption that flow through these zones carries nearly all the flow. Compared to the RCF3 pumping simulations the shaft has to be brought to atmospheric pressure in those points that intersect the zones above the water table in the shaft. In simulations the zone-shaft intersections above 640 m were brought to atmospheric pressure and this information was included/superimposed into a new background/initial head distribution. The constant head interior boundary conditions have been gradually changed downwards (sink rate 1.25m/day; initial head distribution for each transient constant head test is the final distribution of the previous test plus new atmospheric pressure volumes). In those observation points where the zones intersect the borehole RCF3 and the shaft between 640–680 m transient drawdown data and flow rate data have been calculated (the effect of changing the inner hydraulic boundary conditions from that caused by the RCF3 borehole). The cross-sectional area of the shaft is over 50 times larger than the cross-sectional area of RCF3 and although we have calibrated the model parameters against the measured flow in borehole PCF3 we have not included the increased cross-sectional area of the shaft to the calculated results presented in Table A2-II and Figures A2-4…A2-5. In addition to this there might be other changes due to blasting, degassing, drying, stress changes etc.). Simultaneouly the pressure/head changes in adjacent boreholes RCM1 and RCM2 have been calculated and presented in Table A2-III and Figures A2-6…A2-9.

Our prediction measures are summarized in Tables A2-II…A2-III and Figures A2-4…A2-9. The given flow rates into shaft are our best estimates without including any excavation effects.

***Table A2-II.*** *Magnitude of water inflow to section 640…680 m bOD within Sector 7 of shaft.*

| **WINDOW 1: 640 - 660 m bOD**<br>sink rate 1.25 m/day<br>start at depth 640 m bOD<br>end at depth 660 m bOD | | | | | **WINDOW 2: 660 - 680 m bOD**<br>sink rate 1.25 m/day<br>start at depth 660 m bOD<br>end at depth 680 m bOD | |
|---|---|---|---|---|---|---|
| TIME (day) | INFLOW (l/min) | TIME (day) | INFLOW (l/min) | | TIME (day) | INFLOW (l/min) |
| 0 | 0 | | | | 16 | 0 |
| 1 | 0,019799 | 17 | 0,035352 | | 17 | 0,028522 |
| 2 | 0,027415 | 18 | 0,034701 | | 18 | 0,039048 |
| 3 | 0,026022 | 19 | 0,034206 | | 19 | 0,036399 |
| 4 | 0,026092 | 20 | 0,033837 | | 20 | 0,035889 |
| 5 | 0,026383 | 21 | 0,033470 | | 21 | 0,035816 |
| 6 | 0,026997 | 22 | 0,033184 | | 22 | 0,036135 |
| 7 | 0,027697 | 23 | 0,032957 | | 23 | 0,036558 |
| 8 | 0,028556 | 24 | 0,032731 | | 24 | 0,037178 |
| 9 | 0,029343 | 25 | 0,032476 | | 25 | 0,037848 |
| 10 | 0,030220 | 26 | 0,032254 | | 26 | 0,038613 |
| 11 | 0,031067 | 27 | 0,032066 | | 27 | 0,039350 |
| 12 | 0,031983 | 28 | 0,031880 | | 28 | 0,040150 |
| 13 | 0,032860 | 29 | 0,031729 | | 29 | 0,040954 |
| 14 | 0,033819 | 30 | 0,031577 | | 30 | 0,041792 |
| 15 | 0,034718 | 31 | 0,031431 | | 31 | 0,042587 |
| 16 | 0,035643 | 32 | 0,031317 | | 32 | 0,043469 |
| | | steady state at depth 680 m | 0,016457 | | steady state at depth 680 m | 0,021905 |

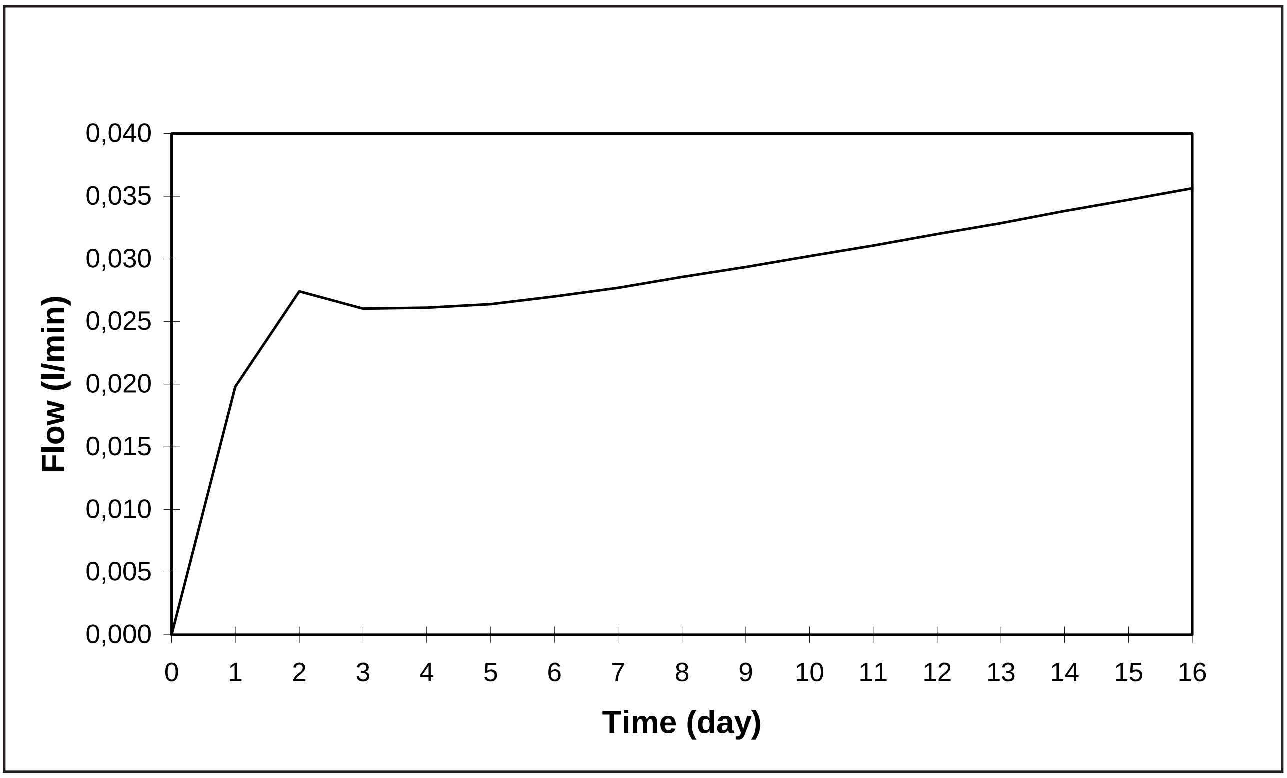


***Figure A2-4.*** *Magnitude of water inflow to shaft. Window 1; 640…660m bOD.*

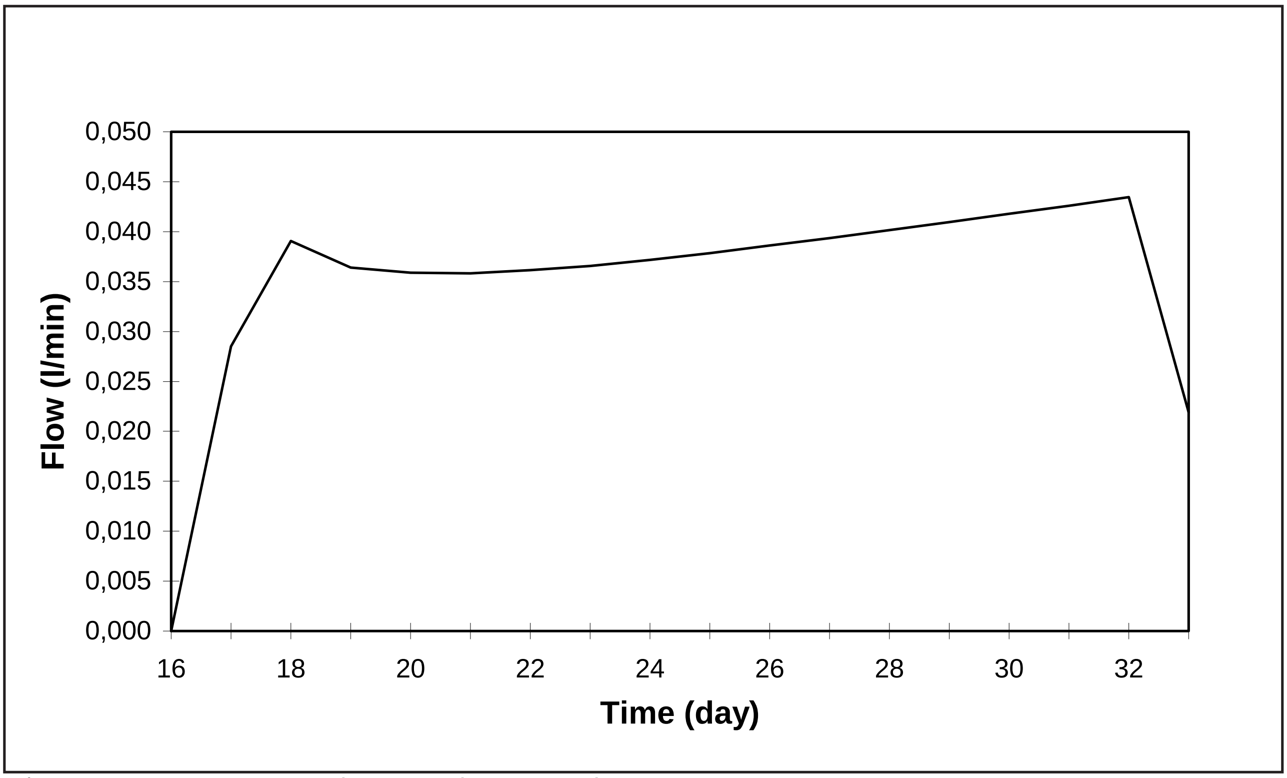


***Figure A2-5.*** *Magnitude of water inflow to shaft. Window 1; 660…680m bOD.*

## APPENDIX 2

PART II: VTT FLOW PREDICTION

***Table A2-III.*** *Changes in water pressure in adjacent boreholes RCM1 and RCM2.*

| Depth (m bOD) | Time (day) | RCM1 640 m bOD | RCM1 680 m bOD | RCM2 640 m bOD | RCM2 680 m bOD |
|---|---|---|---|---|---|
| 600,00 | 0 | 0,001 | 0,001 | 0,001 | 0,001 |
| 601,25 | 1 | 0,001 | 0,001 | 0,001 | 0,001 |
| 602,50 | 2 | 0,001 | 0,001 | 0,001 | 0,001 |
| 603,75 | 3 | 0,001 | 0,001 | 0,001 | 0,001 |
| 605,00 | 4 | 0,001 | 0,001 | 0,001 | 0,001 |
| 606,25 | 5 | 0,001 | 0,001 | 0,001 | 0,001 |
| 607,50 | 6 | 0,001 | 0,001 | 0,001 | 0,001 |
| 608,75 | 7 | 0,001 | 0,001 | 0,001 | 0,001 |
| 610,00 | 8 | 0,001 | 0,001 | 0,001 | 0,001 |
| 611,25 | 9 | 0,001 | 0,001 | 0,001 | 0,001 |
| 612,50 | 10 | 0,001 | 0,001 | 0,001 | 0,001 |
| 613,75 | 11 | 0,001 | 0,001 | 0,001 | 0,001 |
| 615,00 | 12 | 0,001 | 0,001 | 0,001 | 0,001 |
| 616,25 | 13 | 0,001 | 0,001 | 0,001 | 0,001 |
| 617,50 | 14 | 0,001 | 0,001 | 0,001 | 0,001 |
| 618,75 | 15 | 0,001 | 0,001 | 0,001 | 0,001 |
| 620,00 | 16 | 0,001 | 0,001 | 0,001 | 0,001 |
| 621,25 | 17 | 0,001 | 0,001 | 0,001 | 0,001 |
| 622,50 | 18 | 0,001 | 0,001 | 0,001 | 0,001 |
| 623,75 | 19 | 0,001 | 0,001 | 0,001 | 0,001 |
| 625,00 | 20 | 0,001 | 0,001 | 0,001 | 0,001 |
| 626,25 | 21 | 0,001 | 0,001 | 0,001 | 0,001 |
| 627,50 | 22 | 0,001 | 0,001 | 0,001 | 0,001 |
| 628,75 | 23 | 0,001 | 0,001 | 0,001 | 0,001 |
| 630,00 | 24 | 0,001 | 0,001 | 0,001 | 0,001 |
| 631,25 | 25 | 0,001 | 0,001 | 0,001 | 0,001 |
| 632,50 | 26 | 0,001 | 0,001 | 0,001 | 0,001 |
| 633,75 | 27 | 0,001 | 0,001 | 0,001 | 0,001 |
| 635,00 | 28 | 0,001 | 0,001 | 0,001 | 0,001 |
| 636,25 | 29 | 0,001 | 0,001 | 0,001 | 0,001 |
| 637,50 | 30 | 0,001 | 0,001 | 0,001 | 0,001 |
| 638,75 | 31 | 0,001 | 0,001 | 0,001 | 0,001 |
| 640,00 | 32 | 0,001 | 0,001 | 0,001 | 0,001 |
| 641,25 | 33 | 0,001 | 0,001 | 0,001 | 0,001 |
| 642,50 | 34 | 0,001 | 0,001 | 0,001 | 0,001 |
| 643,75 | 35 | 0,001 | 0,001 | 0,001 | 0,001 |
| 645,00 | 36 | 0,001 | 0,001 | 0,001 | 0,001 |
| 646,25 | 37 | 0,001 | 0,001 | 0,001 | 0,001 |
| 647,50 | 38 | 0,001 | 0,001 | 0,001 | 0,001 |
| 648,75 | 39 | 0,001 | 0,001 | 0,001 | 0,001 |
| 650,00 | 40 | 0,001 | 0,001 | 0,001 | 0,001 |
| 651,25 | 41 | 0,001 | 0,001 | 0,001 | 0,001 |
| 652,50 | 42 | 0,001 | 0,001 | 0,001 | 0,001 |
| 653,75 | 43 | 0,118 | 0,001 | 0,001 | 0,001 |
| 655,00 | 44 | 0,118 | 0,001 | 0,001 | 0,001 |
| 656,25 | 45 | 0,236 | 0,001 | 0,001 | 0,001 |
| 657,50 | 46 | 0,236 | 0,001 | 0,001 | 0,001 |
| 658,75 | 47 | 0,354 | 0,001 | 0,001 | 0,001 |
| 660,00 | 48 | 0,854 | 0,001 | 0,118 | 0,001 |
| 661,25 | 49 | 0,972 | 0,001 | 0,118 | 0,001 |
| 662,50 | 50 | 1,090 | 0,001 | 0,118 | 0,001 |
| 663,75 | 51 | 1,453 | 0,001 | 0,118 | 0,001 |
| 665,00 | 52 | 1,954 | 0,001 | 0,147 | 0,001 |
| 666,25 | 53 | 2,072 | 0,001 | 0,177 | 0,001 |
| 667,50 | 54 | 2,308 | 0,001 | 0,177 | 0,001 |
| 668,75 | 55 | 2,936 | 0,001 | 0,216 | 0,001 |
| 670,00 | 56 | 3,290 | 0,029 | 0,579 | 0,001 |
| 671,25 | 57 | 3,800 | 0,029 | 0,648 | 0,001 |
| 672,50 | 58 | 4,154 | 0,059 | 0,697 | 0,001 |
| 673,75 | 59 | 4,782 | 0,059 | 0,766 | 0,001 |
| 675,00 | 60 | 5,018 | 0,098 | 1,129 | 0,001 |
| 676,25 | 61 | 5,254 | 0,128 | 1,198 | 0,001 |
| 677,50 | 62 | 6,000 | 0,491 | 1,228 | 0,001 |
| 678,75 | 63 | 6,354 | 0,609 | 1,336 | 0,029 |
| 680,00 | 64 | 6,864 | 0,648 | 1,699 | 0,029 |
| steady state | | 174,344 | 189,614 | 154,74 | 171,82 |

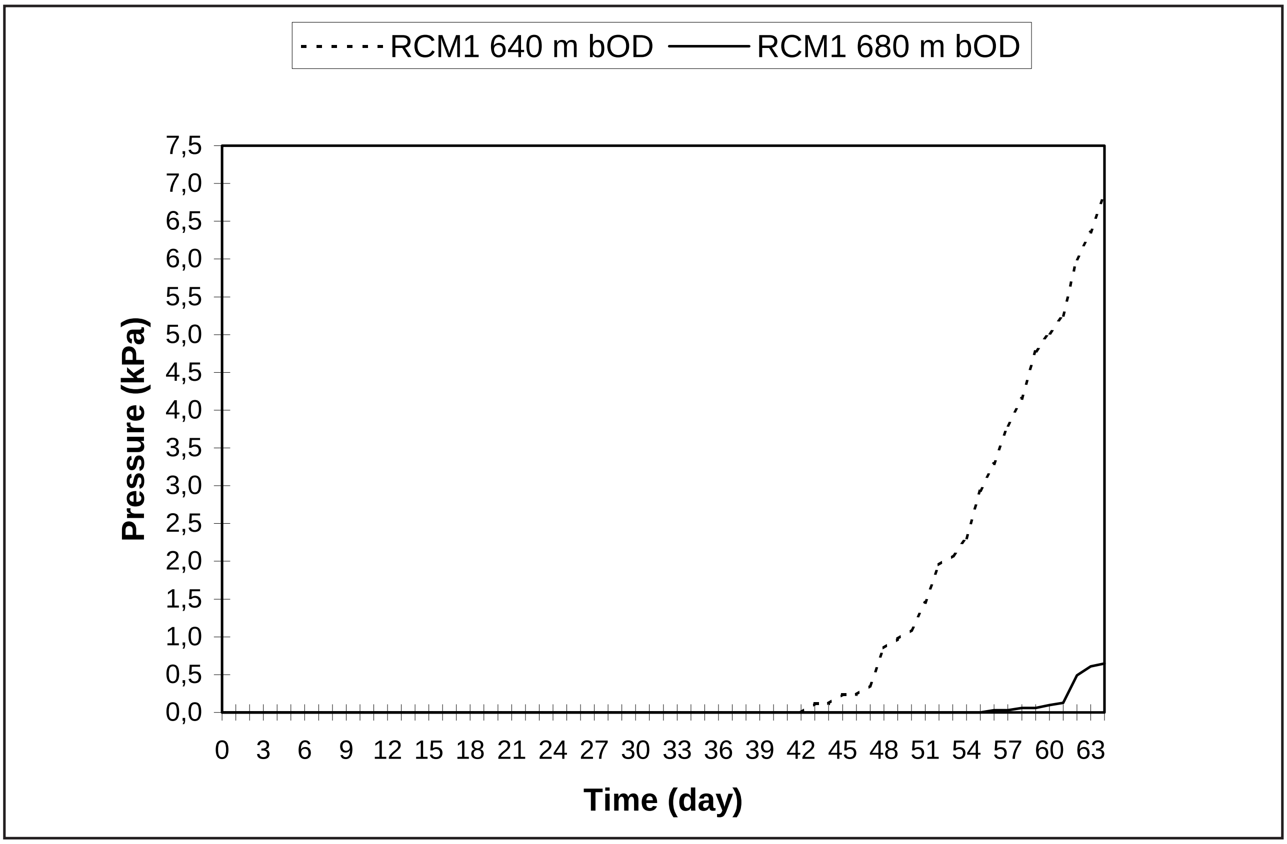


***Figures A2-6.*** *Pressure change in borehole RCM1 at depths of 640 m and 680 m bOD. Monitoring time 64 days.*

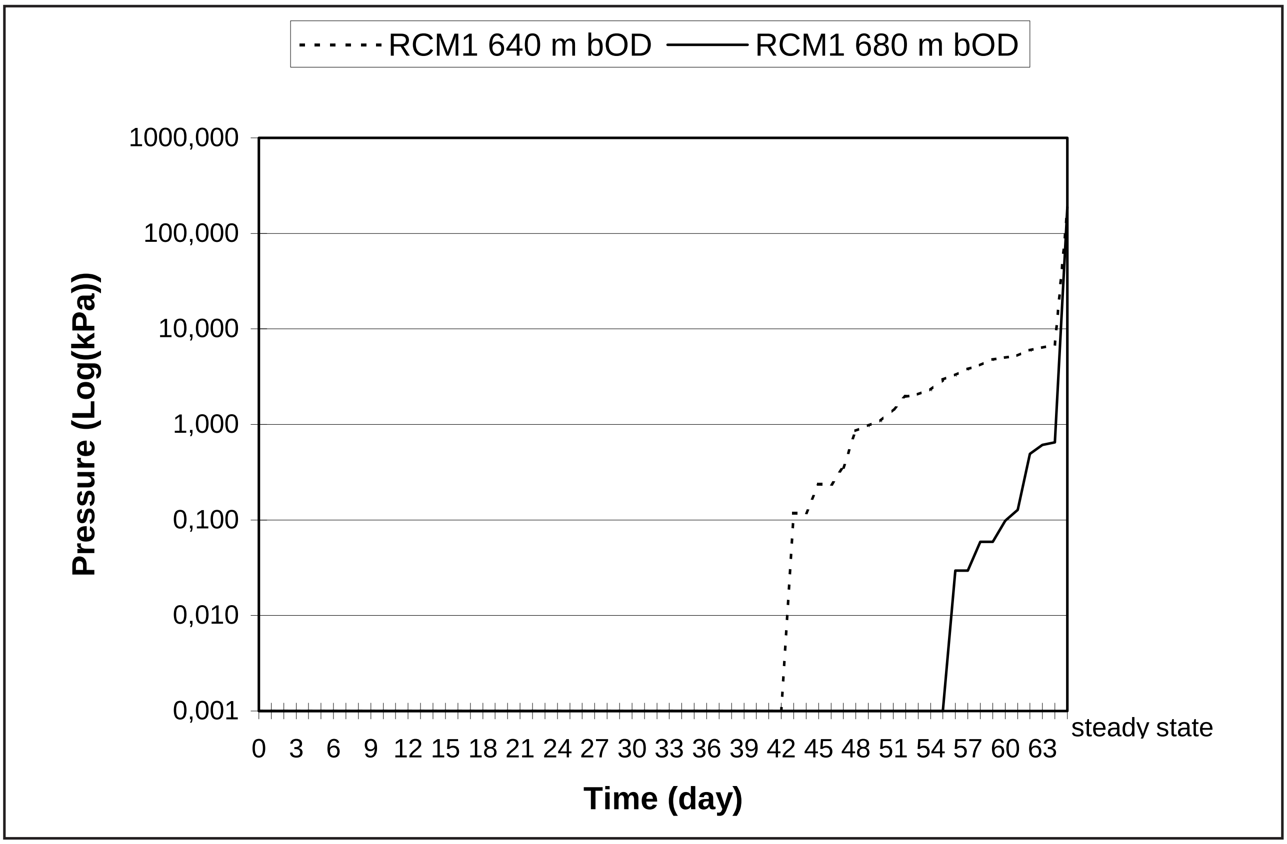


***Figure A2-7.*** *Pressure change in borehole RCM1 at depths of 640 m and 680 m bOD. Monitoring to steady state.*

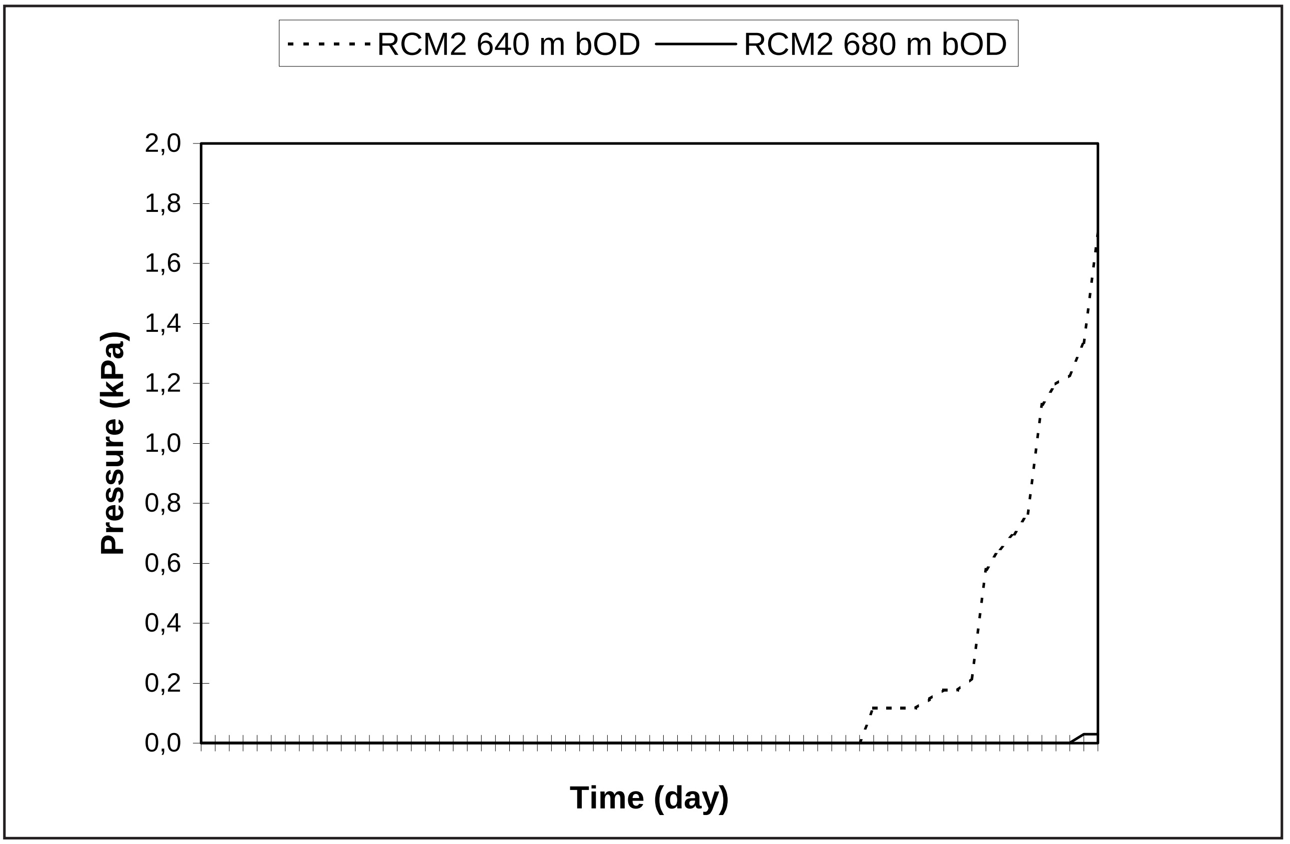


***Figure A2-8.*** *Pressure change in borehole RCM 2 at depths of 640 m and 680 m bOD. Monitoring time 64 days.*

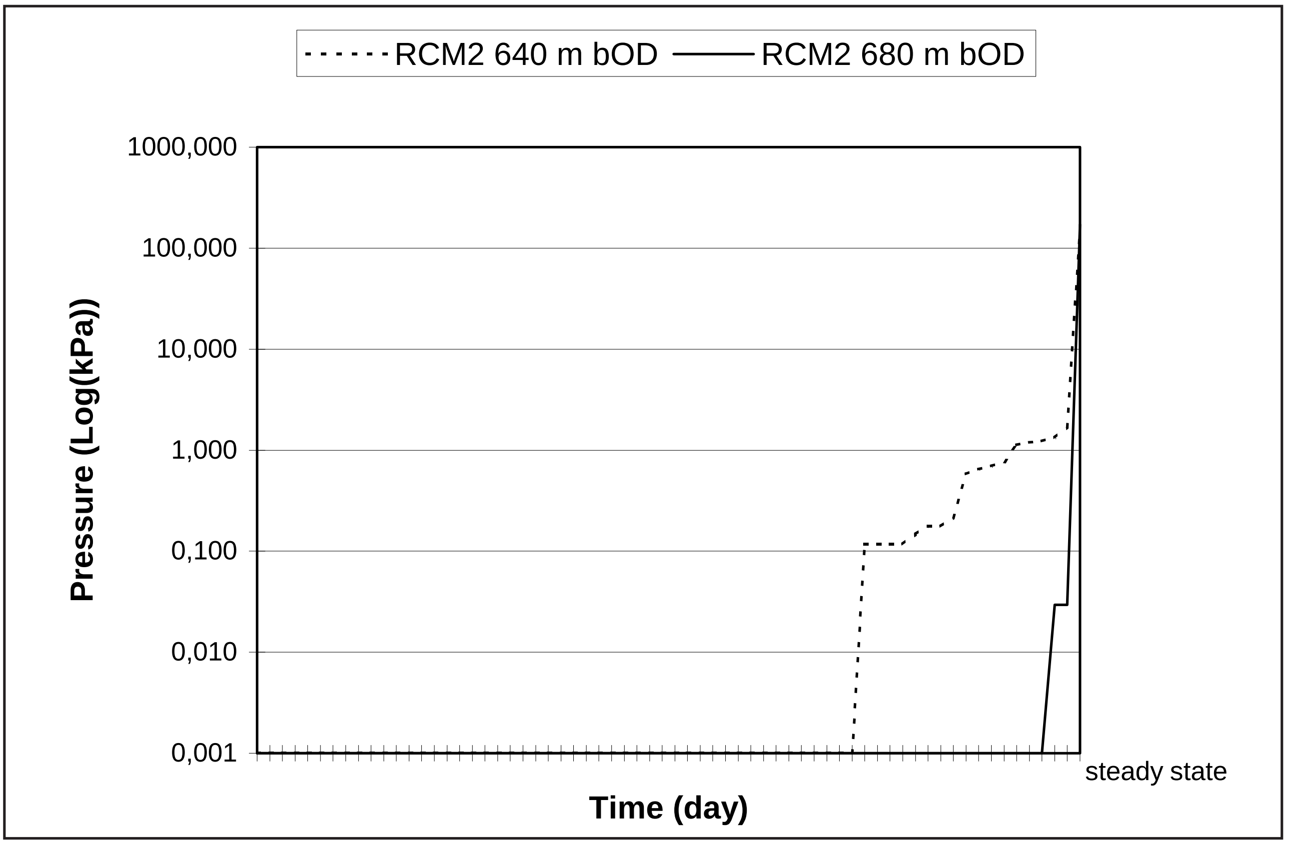


***Figure A2-9.*** *Pressure change in borehole RCM2 at depths of 640 m and 680 m bOD. Monitoring to steady state.*

# A2-6 Conclusions

With the applied finite-element flow code, TRINET, simulation of flow and transport can be produced in discretely fractured or equivalent continuum aquifers/porous medium, or in any combination of discrete and continuum aquifers. Therefore the quality of the presented predictions depends almost completely on how well we have succeeded in our conceptual modelling of the flow system.

In this study the Sellafield hydrology has been simplified to include only the deterministic major water-conducting features/zones and discontinuum approach has been used to model flow. The fracture zone-dominating flow is characteristic in Finnish crystalline bedrock, especially below 150-200 m depth, and even if the absolute, deterministic zone model may not be the best approach in Sellafield case, the presented study serves at least as a general presentation of our modelling approach. The constant material values have been assigned to each deterministic structure and these parameter values as well as outer boundary conditions have been calibrated by adjusting conductivities, storativities etc. to meet the head and flow conditions of the RCF3 pumping test. Because the evaluated hydraulic properties are derived only from a single interference test, they represent effective values within large influence radius and it is likely that our simplified description is too simplified to describe the detailed flow reality. Correct selection of boundary conditions is even more critical step in model design than averaging the parameters. Especially in steady-state simulations, the boundaries largely determine the flow pattern. The analysis of presented results against the previous flow measurements also indicate that our straightforward approach to connect the interesting shaft section to the zone system simply through parallel zones oversimplifies the hydraulic flow conditions around the shaft and more detailed conceptualization would improve predictions.

# A2-7 References

Birkholzer, J., and Karasaki, K, 1995. FMGN, RENUMN, POLY, TRIPOLY: Chain of Programs for calculating and analyzing flow and transport in fracture networks embedded in porous matrix blocks. Theory, Design and User's Manual. Lawrence Berkeley Laboratory Report, 50p.

Doughty, C., 1995. Estimation of Hydrologic Properties of Heterogeneous Media with an Inverse Method Based on Iterated Function Systems. Lawrence Berkeley Laboratory Report, LBC-38136, p. 257.

Ijiri, Y., and Karasaki, K., 1994. A Lagrangian-Eulerian Finite Element Method with Adaptive Gridding for Advection-Dispersion Problems. Lawrence Berkeley Laboratory, University of California. Report LBL-35224, 15p.

Karasaki, K., 1986. Well test analysis in fractured media. PhD Thesis, University of California at Berkley. 239 p.

Karasaki, K., 1987. A new advection-dispersion code for calculating transport in fracture networks. In: Earth Sci. Div. Lawrence Berkley Laboratory Annual Report 1986 LBL-22090, pp. 55–57

Karasaki, K., 1988. Modification to TRINET: A three-dimensional advection-dispersion code for fracture networks. In: Earth Sci. Div. Lawrence Berkley Laboratory Annual Report 1987 LBL-24200, pp. 175–176.

Korkealaakso, J. and Kontio, K., 1995. Characterization of fracture zones by inverse analysis of interference tests. SKB Äspö Hard Rock Laboratory: International Cooperation Report 96-02. 53 p.

Nirex, 1993. Geology and Hydrogeology of the Sellafield Area. Nirex report no 524.

Nirex, 1993. Scientific Update 1993. Nirex report no: 525.

Nirex, 1995. Science Report. Sellafield Geological Investigations. The 3D geological structure of the PRZ. Report no: S/95/005.

Nirex, 1995. Science Report. Sellafield Geological and Hydrogeological Investigations. The 3D geology and hydrogeology of the RCF south shaft location. Report no: S/95/007.

Segan, S. and Karasaki, K., 1993. TRINET: A flow and transport code for fracture networks—User´s manual and tutorial, Lawrence Berkeley Laboratory report, Berkeley, CA. 57 p.